Ion Kinetics at the Plasma Material Interface in Oblique Magnetic Fields

Davide Curreli

Department of Nuclear, Plasma, and Radiological Engineering
University of Illinois at Urbana Champaign

dcurreli@illinois.edu

Multiscale, interlinked PSI phenomena

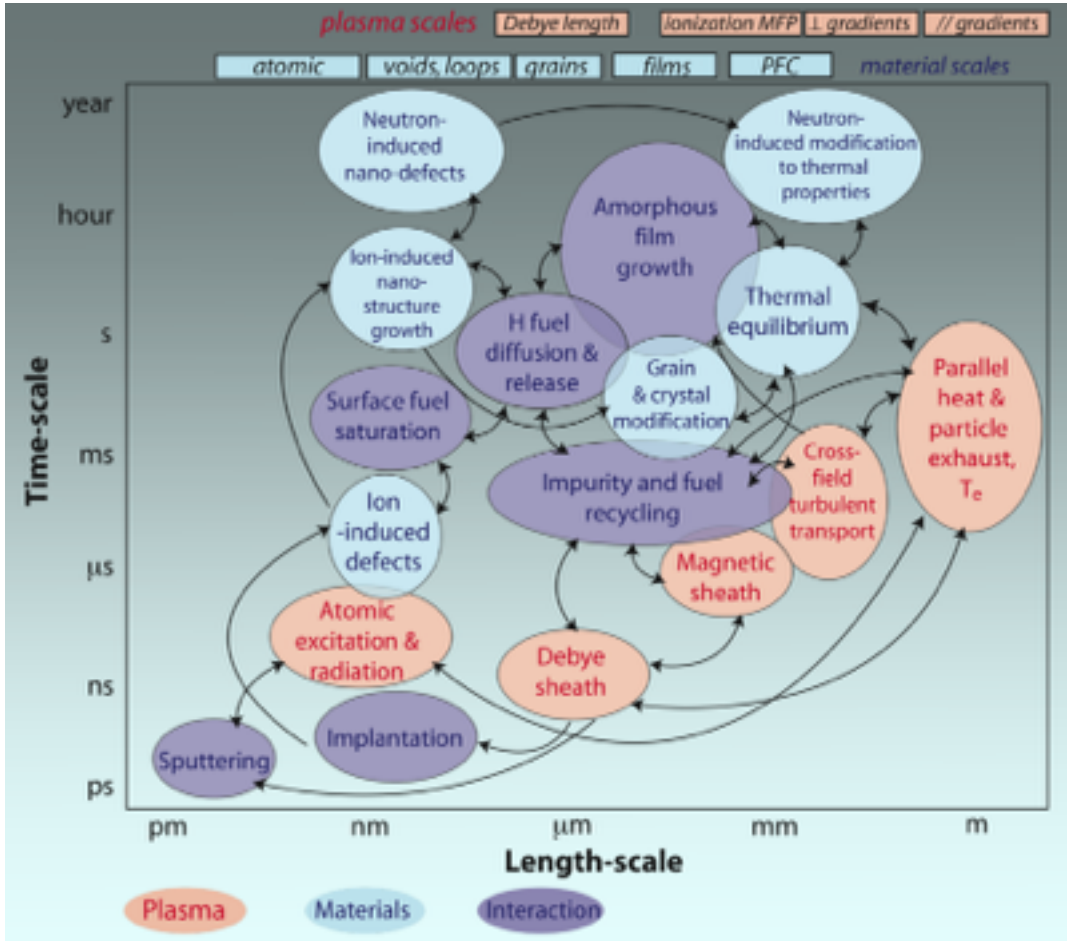

* Wirth, Nordlund, Whyte, and Xu, *Materials Research Society Bulletin* **36** (2011) 216-222

Multiscale, interlinked PSI phenomena

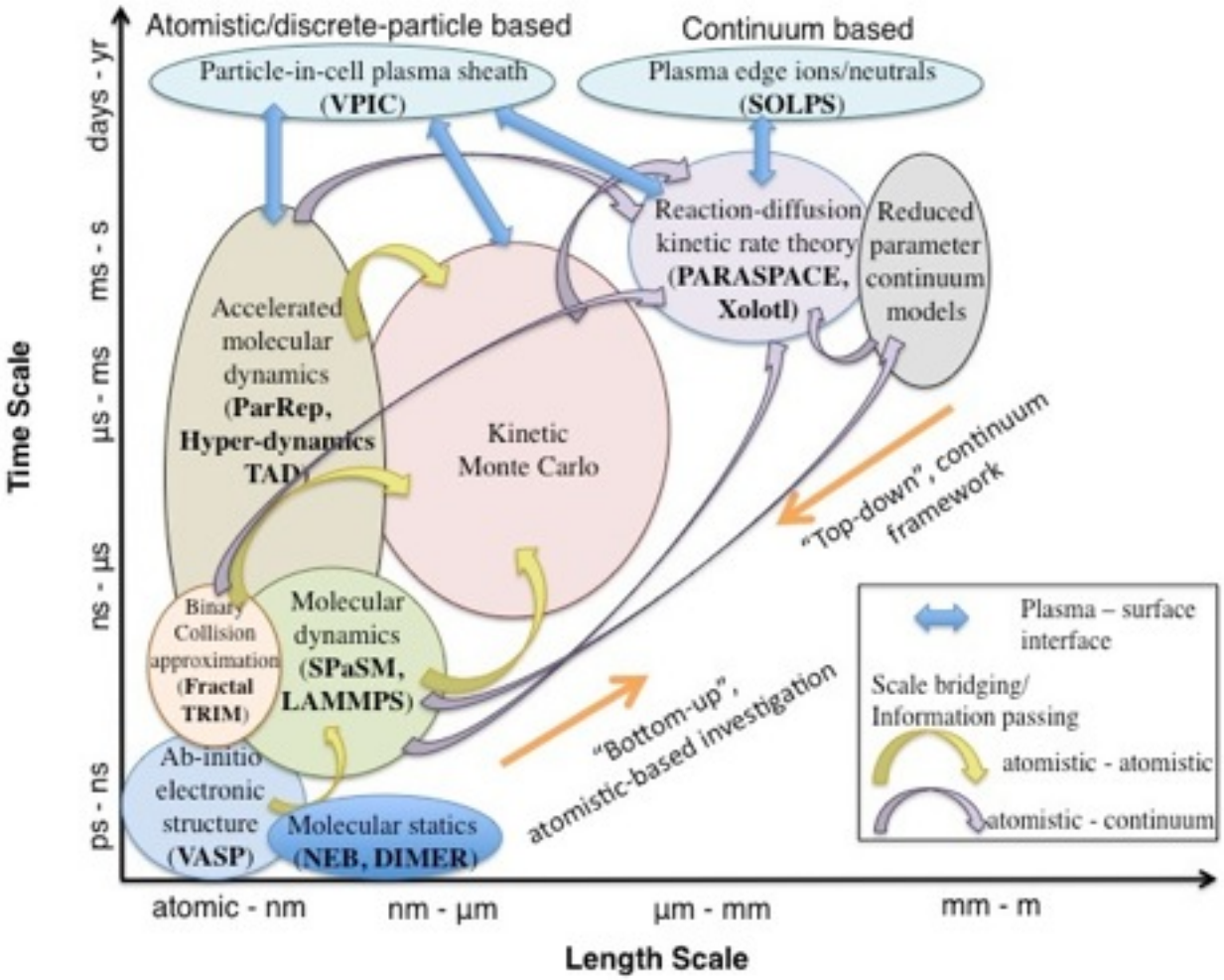

Feedback Loop of Plasma Sheath & Material Release

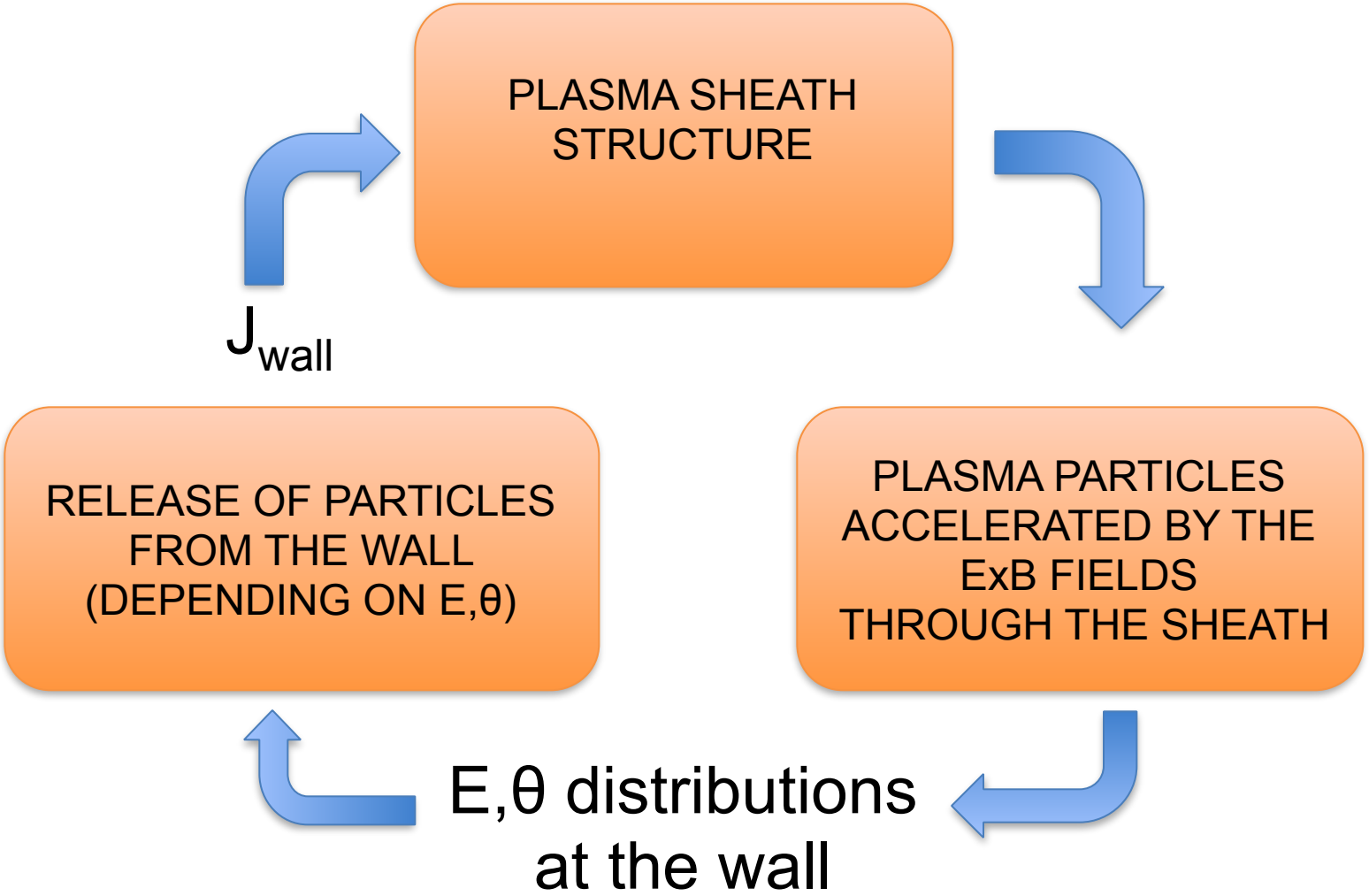

Outline

- Ion distribution functions at the material wall of a magnetized plasma
  - Fluid model
  - PIC model
- Wall response
  - BCA methods for material properties
  - Development of Fractal-TRIDYN
- Coupling methodologies with fluid-kinetic codes
  - SOLPS, EMC3, EIRENE
  - Using only the “relevant” information

A Simple Question

What is the <u>energy</u> and the <u>angle</u> of plasma ions at the boundary of a magnetized plasma?

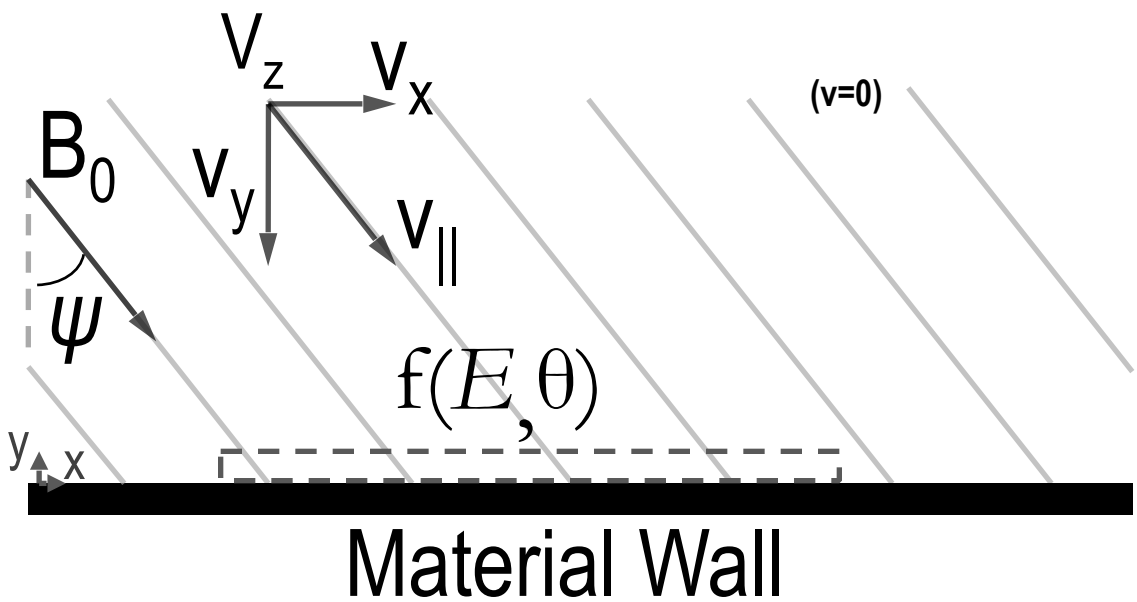

Release of Material Particles (e.g. Y, δ_e) and wall reflection coefficients depend on $f(E,\theta)$ @ wall. E.g.: $SY(E,\theta)$

E

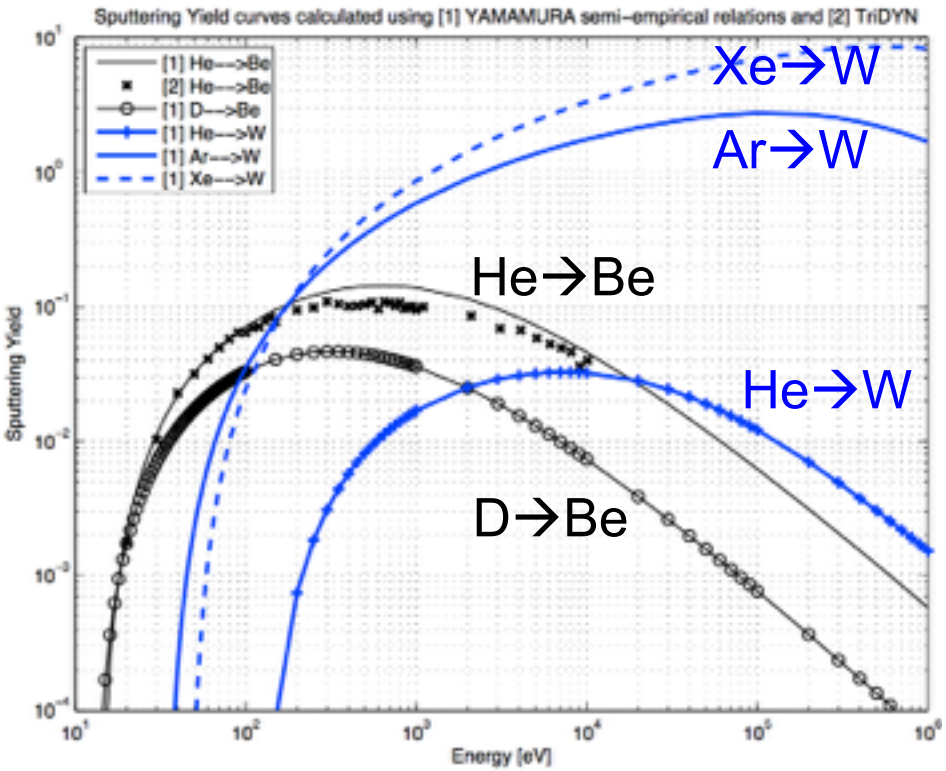

θ

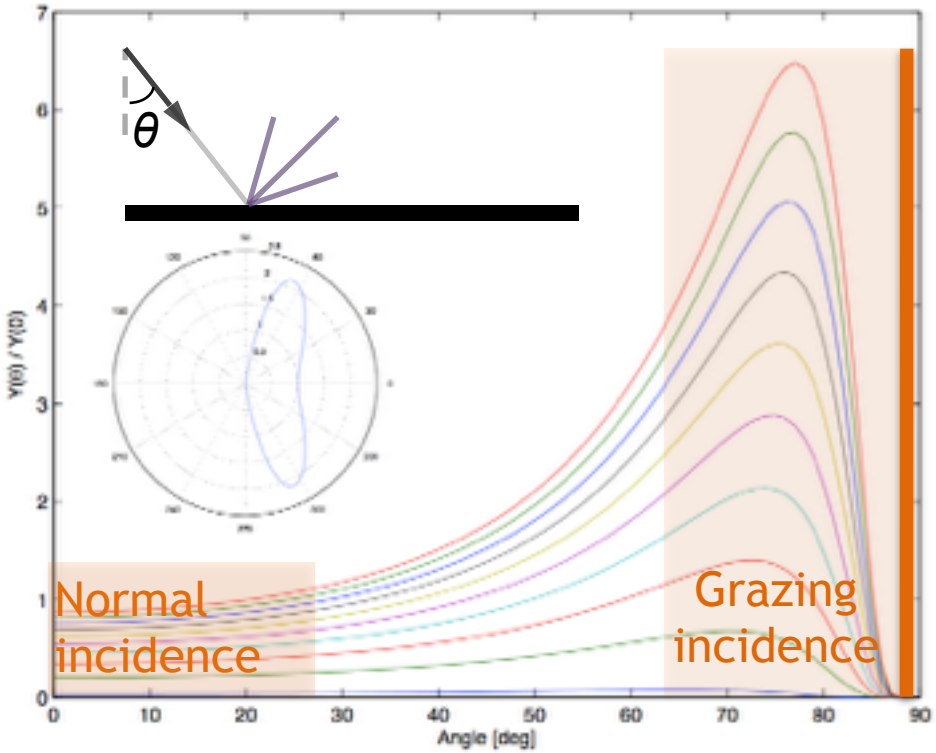

Classical picture of the Magnetized Plasma Sheath

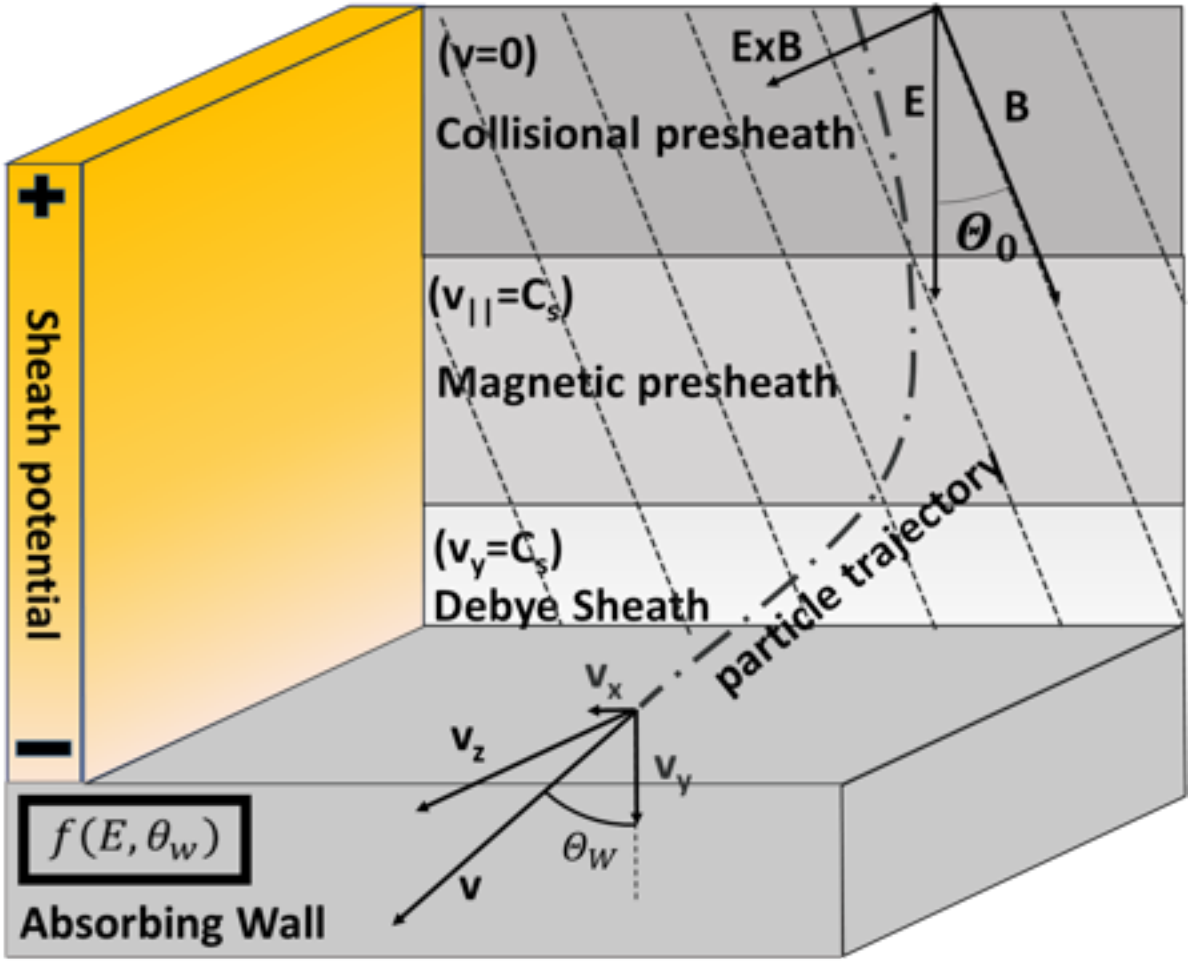

Ion Energy-Angle Distribution Function

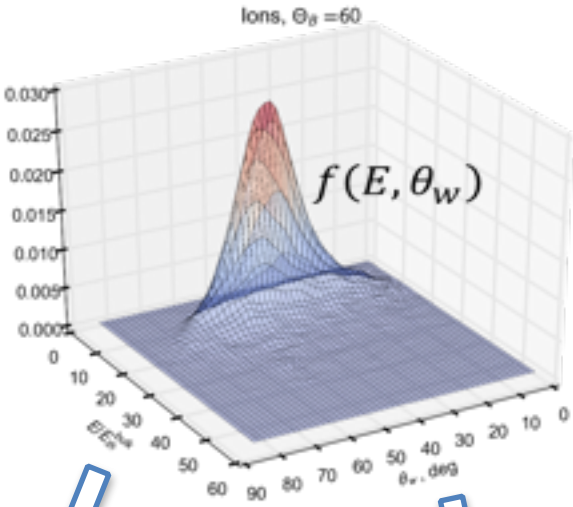

Marginal distributions derived from f(E,θ)

$$f_{E_w}(E) = \int_0^{\pi/2} d\theta\, f(E,\theta)$$

$$f_{\theta_w}(\theta) = \int_0^{\infty} dE\, f(E,\theta)$$

Models of the Magnetized Sheath

Authors (list of selected works)	Fluid Model	Kinetic Model
Chodura, Phys. Fluids 25, 1628 (1982)		**x (pic)**
A.B. DeWald, A.W. Bailey, J.N. Brooks, Phys. Fluids 30, 267 (1987)		**x (pic)**
K-U. Riemann, J. Phys. D: Appl. Phys. 24 493-518 (1991) K-U. Riemann, PoP 1, 552 (1994) K-U. Riemann PoP 4, 4158 (1997)	**x**	
P. C. Stangeby, PoP 2, 702 (1995)	**x**	
E. Ahedo, PoP 4, 12 (1997)	**x**	
G. Manfredi et al, Comp. Phys. Comm. 164, 262-268 (2004) S. Devaux and G. Manfredi, Phys. Plasmas 13, 083504 (2006) G. Manfredi and S. Devaux, AIP Conf. Proc. 1061, 178 (2008)		**x (Vlasov)**
G. Kawamura and A. Fukuyama, PoP, 14, 083502 (2007)		**x (gyrokin)**
T.M.G. Zimmermann et al, PoP 15, 072301 (2008)	**x**	
P. C. Stangeby, NF, 2012	**x**	

Riemann Fluid Model including fluid Collisions and Ionization

1. Continuity
2. Momentum
3. Isothermal ideal-gas EoS
4. Quasi-neutrality
5. Boltzmann electrons

$$\nabla \cdot (n_i \vec{v}) = n_e \nu_{iz}$$

$$n_i M_i (\vec{v} \cdot \nabla)\vec{v} = n_i q_e (\vec{E} + \vec{v} \times \vec{B}) - \nabla p_i - M_i n_i \nu_t \vec{v}$$

$$p_i = k_B T_i n_i$$

$$n_i = n_e = n_0 \exp\left(\frac{e\phi}{k_B T_e}\right)$$

Dimensionless variables

$$X = \frac{x}{\lambda_{\mathrm{mfp}}}; \quad V = \frac{v}{c_s}; \quad \phi = -\frac{eU}{k_B T_e},$$

$$\Delta = \frac{\nu_i}{\nu_t}; \quad \lambda_{\mathrm{mfp}} = \frac{c_s}{\nu_t}; \quad \omega\tau = \frac{eB}{m_i \nu_t},$$

$$\alpha = \frac{\pi}{2} - \psi$$

$$V_x \frac{dV_y}{dX} = \omega\tau \sin(\alpha) V_z - V_y,$$

$$V_x \frac{dV_z}{dX} = \omega\tau \cos(\alpha) V_x - \omega\tau \sin(\alpha) V_y - V_z,$$

$$\left(V_x - \frac{1}{V_x}\right)\frac{dV_x}{dX} = -\omega\tau \cos(\alpha) V_z - \frac{\Delta}{V_x} - V_x,$$

$$V_x \frac{d\phi}{dX} = \frac{dV_x}{dX} - \Delta.$$

(+B.C.)

Typical profiles from Fluid Model

$\omega_{ci}\,\tau_i = 100$, $\psi = 85$ deg, $\Delta = 0.1$

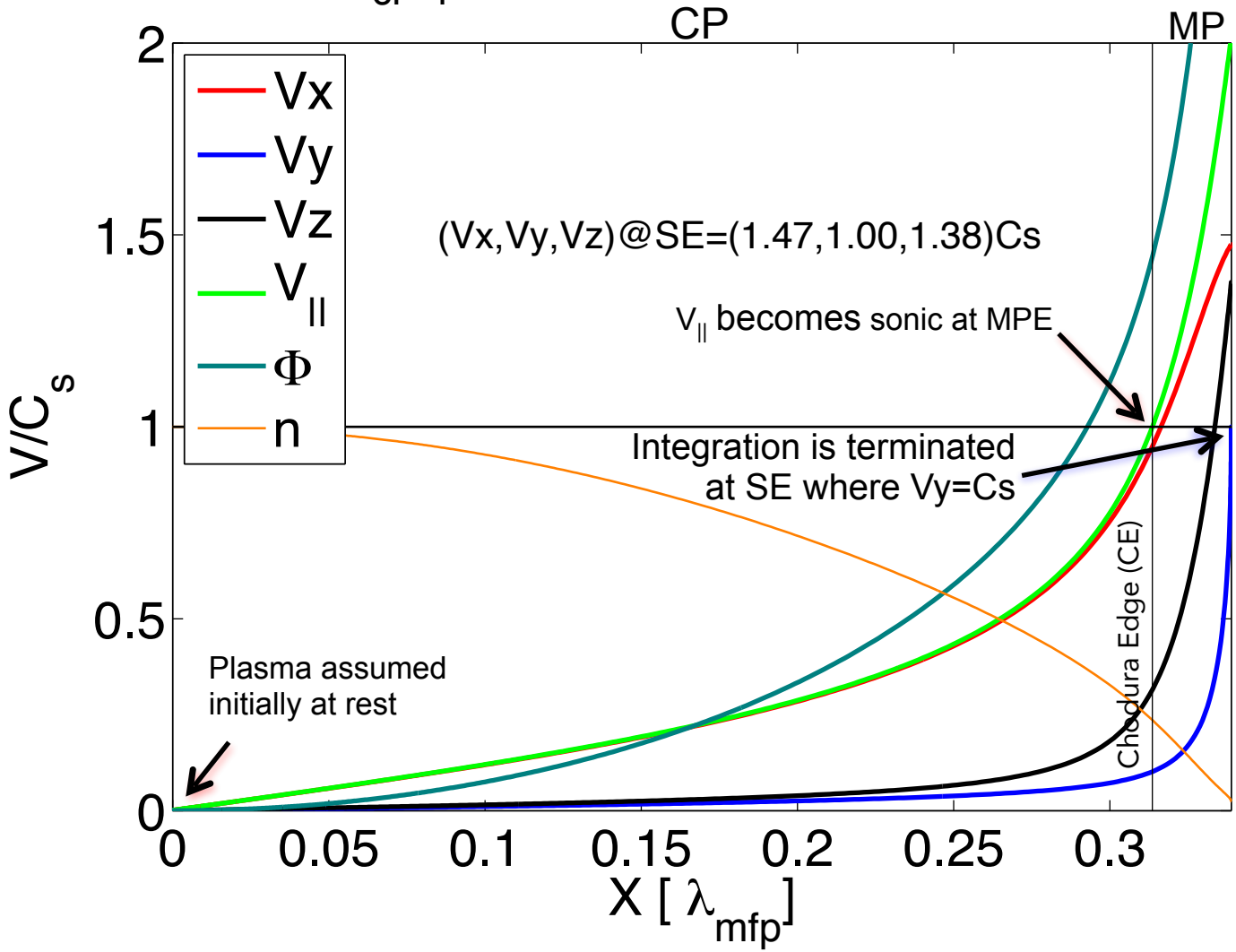

Collisional and Magnetic Presheath structure in Strongly-Magnetized, Weakly-Collisional case

Strongly magnetized, weakly collisional plasma

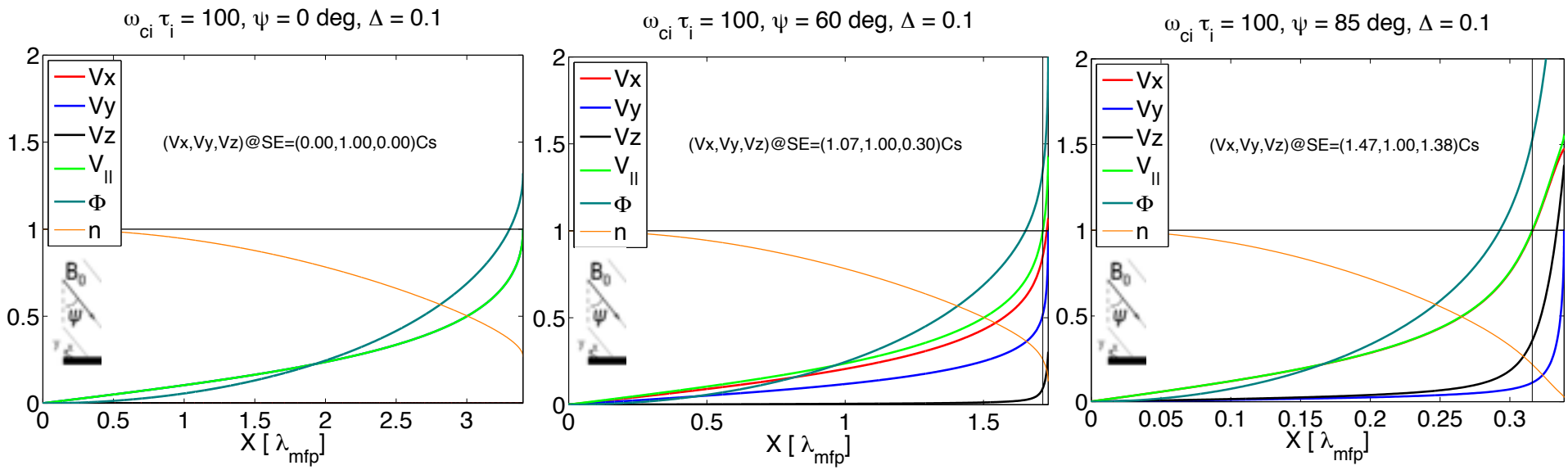

<u>0 deg</u>

- CP only
- No magnetic preheath
- Drift velocity different than zero only in parallel direction, $V_{||}$ =Vy

<u>60 deg</u>

- CP+MP
- Drift velocity has 3D features, with Vx,Vy,Vz all different than zero
- $V_{||}$ gains additional momentum by the presence of the MP, becoming supersonic inside MP, before quasi-neutrality is broken (DS)

<u>85 deg</u>

- CP+MP
- At grazing angles the MP size becomes larger
- $V_{||}$,Vx,Vz are all supersonic
- Interestingly, Vx (parallel to the wall) begins to decrease
- Sheath size decreases with

Ion Drift Velocity at Debye Sheath Entrance depends on the inclination of the B-field

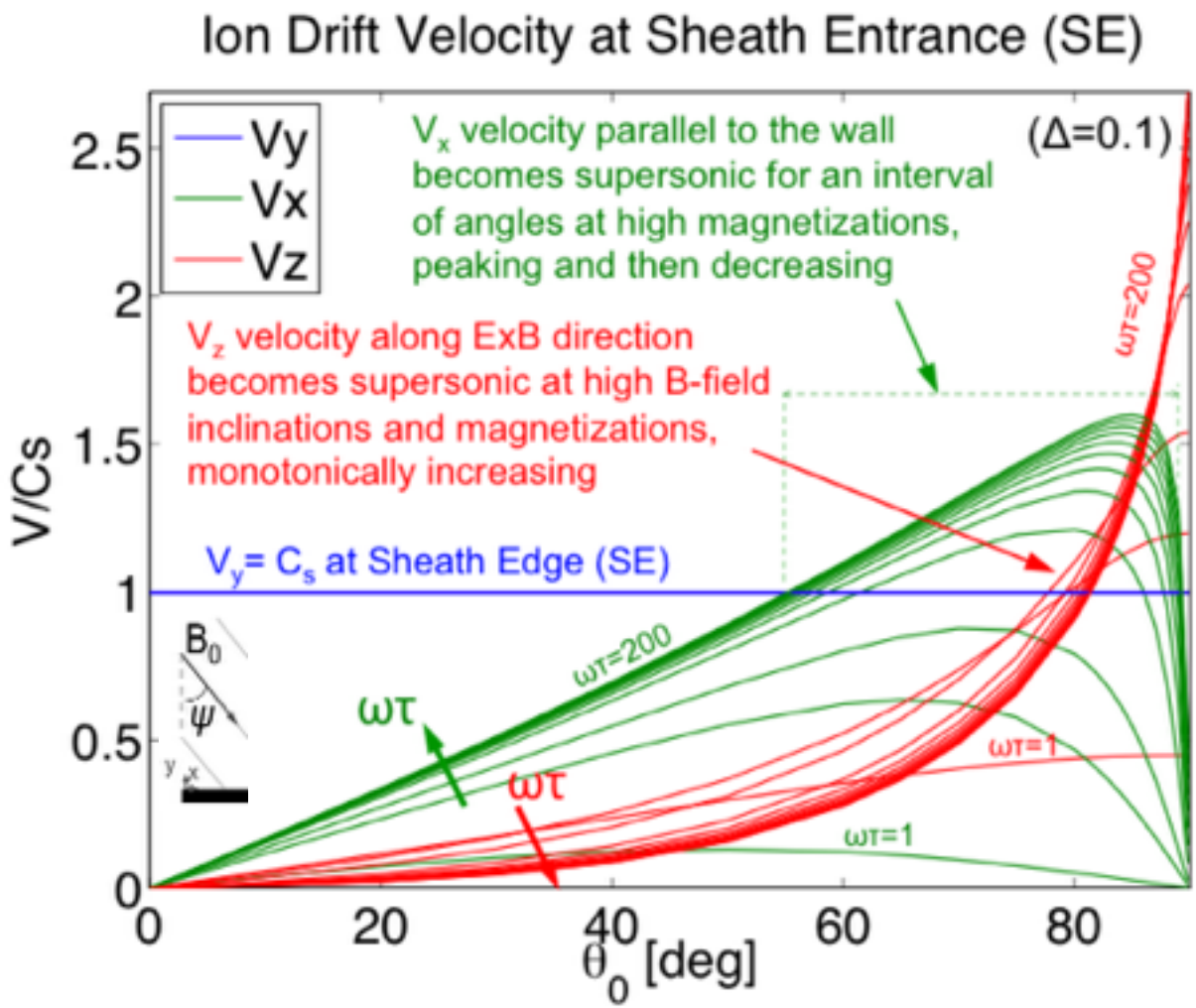

Fluid Kinetic Energy at Debye Sheath Entrance vs. inclination ψ of the B-field

Fluid Ion Kinetic Energy Ei at Sheath Entrance (SE)

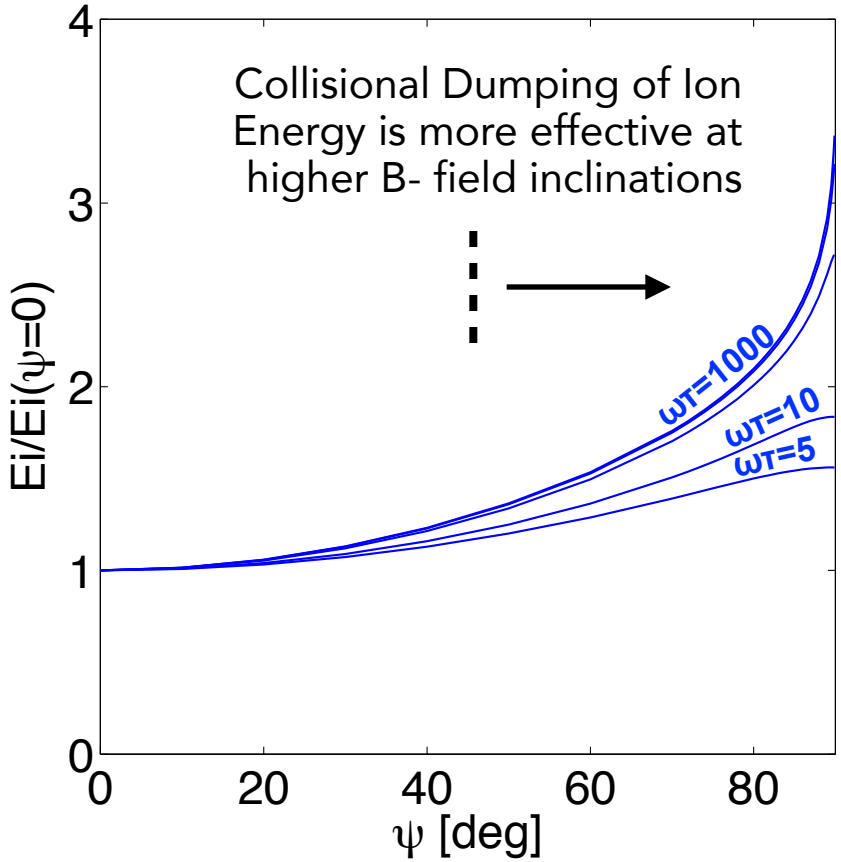

Strong magnetization

Weak magnetization

Collisions provide a mechanism to dissipate ion kinetic energy across the pre-sheaths (CP and MP)

Flow Inclination from Fluid Model

$\omega_{ci}\,\tau_i = 100$, $\psi = 85$ deg, $\Delta = 0.1$

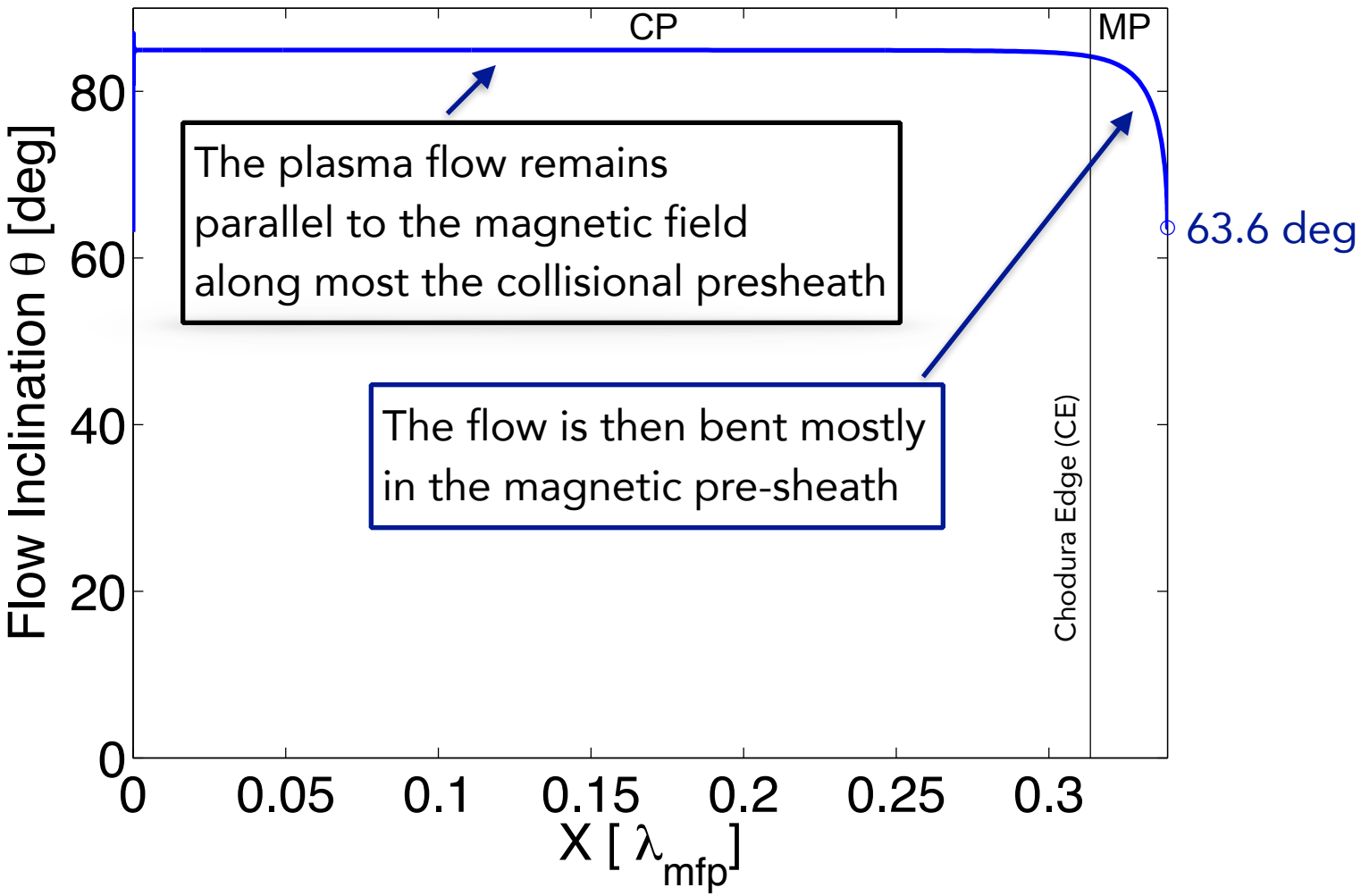

Flow Inclination θ at Debye Sheath Entrance vs. Inclination ψ of the B-field

Flow Inclination θ at Sheath Entrance (SE)

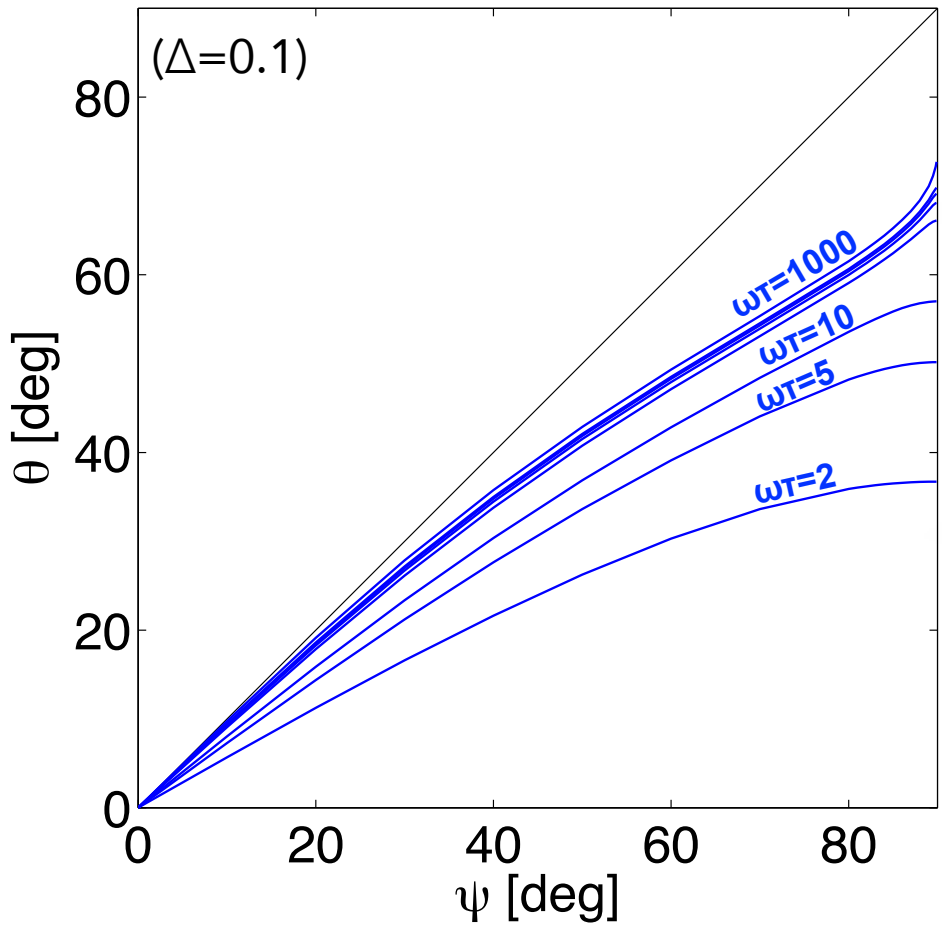

Strong magnetization

Weak magnetization

Collisions provide a mechanism to bend the plasma flow toward normal incidence

Flow Inclination θ at Debye Sheath Entrance vs. Inclination ψ of the B-field

Flow Inclination θ at Sheath Entrance (SE)

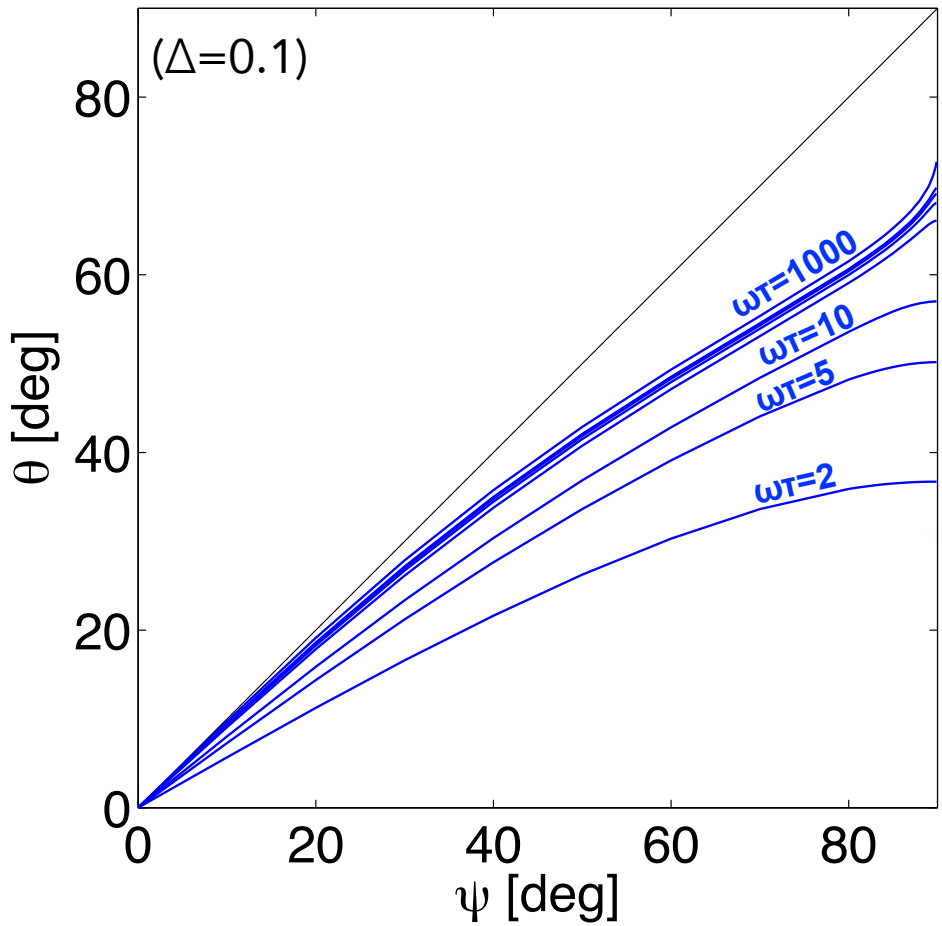

Strong magnetization

Weak magnetization

Collisions provide a mechanism to bend the plasma flow toward normal incidence

$f(E)$ and $f(\theta)$ of a Deuterium Plasma in B_0=1.0 Tesla field, θ_0=30°,45°,60°

ψ=30° ψ=45° ψ=60°

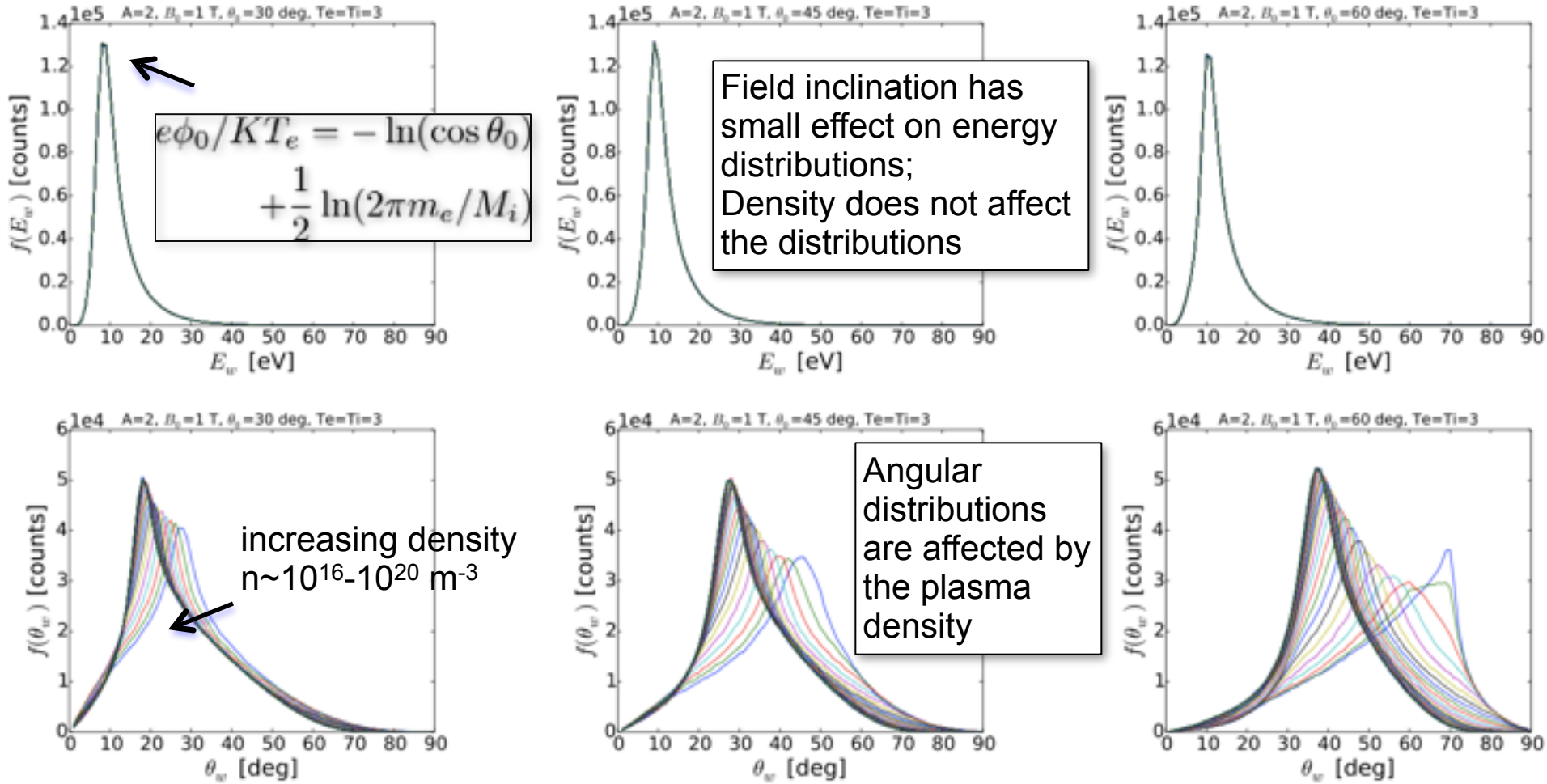

$$e\phi_0/KT_e = -\ln(\cos\theta_0) + \frac{1}{2}\ln(2\pi m_e/M_i)$$

Field inclination has small effect on energy distributions;
Density does not affect the distributions

Angular distributions are affected by the plasma density

A Fully-Kinetic Analysis is Necessary: PIC

- Methodology
  - kinetic-kinetic explicit PIC (kinetic ions, kinetic electrons)
  - electrostatic
  - Particle pusher: Leapfrog, parallelized w/ MPI
  - Field solver: PETSc Multigrid on structured mesh; unstructured mesh also available but not used for plasma sheath analysis
  - MPI: OpenMPI
  - Viz: Paraview, Post-proc: Python
- Simulations
  - 2D3V
  - kinetic ions (10^7), kinetic electrons(10^7), ppc~75
  - dt = (1/20)min(ω_{ce}, ω_{pe}), O(~500 fs)
  - dx = (1/20)min(λ_D,r_L), O(~0.5 μm)
  - B-field inclinations 0,30,60,85 deg
  - Uniform ionization source
  - Lorentz collision operator
    - Collisionless
    - $\omega_{ci} < \nu < \omega_{ce}$
    - $\omega_{ci} < \omega_{ce} < \nu$

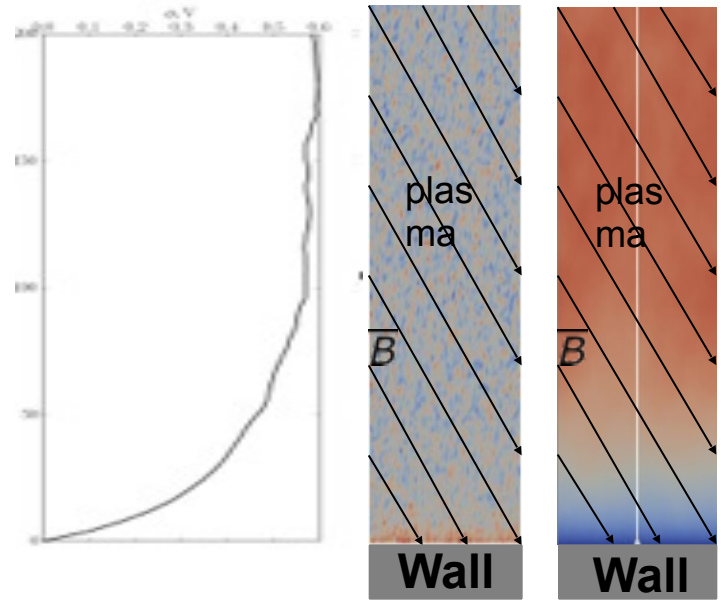

Simulation parameters	
< n	6x10
B	1.0 [T]
θ_B	0,30,60,85 deg
domain size,	~240
# of iterations	~50000
particles per cell	~75

Fluid Moments obtained from the electron and ion particle state-vector

- The qualitative features of the fluid moments agree with the simpler "classical" fluid models (Riemann, Zimmermann, etc.)
- Sheath size decreases with increasing inclination of the B-field
- However, the kinetic simulations reveal that ions and electrons are not isothermal over the domain and electrons are not Boltzmann
- Ion temperature decreases during the acceleration through the CP +MP sheath
- Local deviations from classical fluid models are observed (not today's topic)

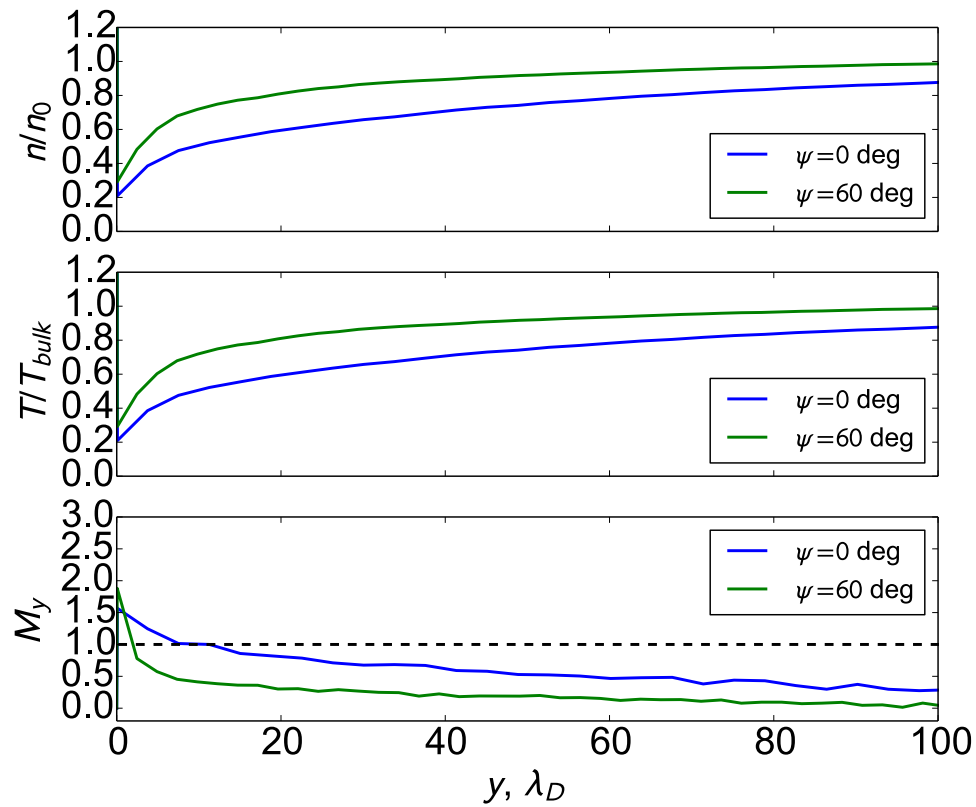

Fluid Moments obtained from the electron and ion particle state-vector

- The qualitative features of the fluid moments agree with the simpler "classical" fluid models (Riemann, Zimmermann, etc.)
- Sheath size decreases with increasing inclination of the B-field
- However, the kinetic simulations reveal that ions and electrons are not isothermal over the domain and electrons are not Boltzmann
- Ion temperature decreases during the acceleration through the CP +MP sheath
- Local deviations from classical fluid models are observed (not today's topic)

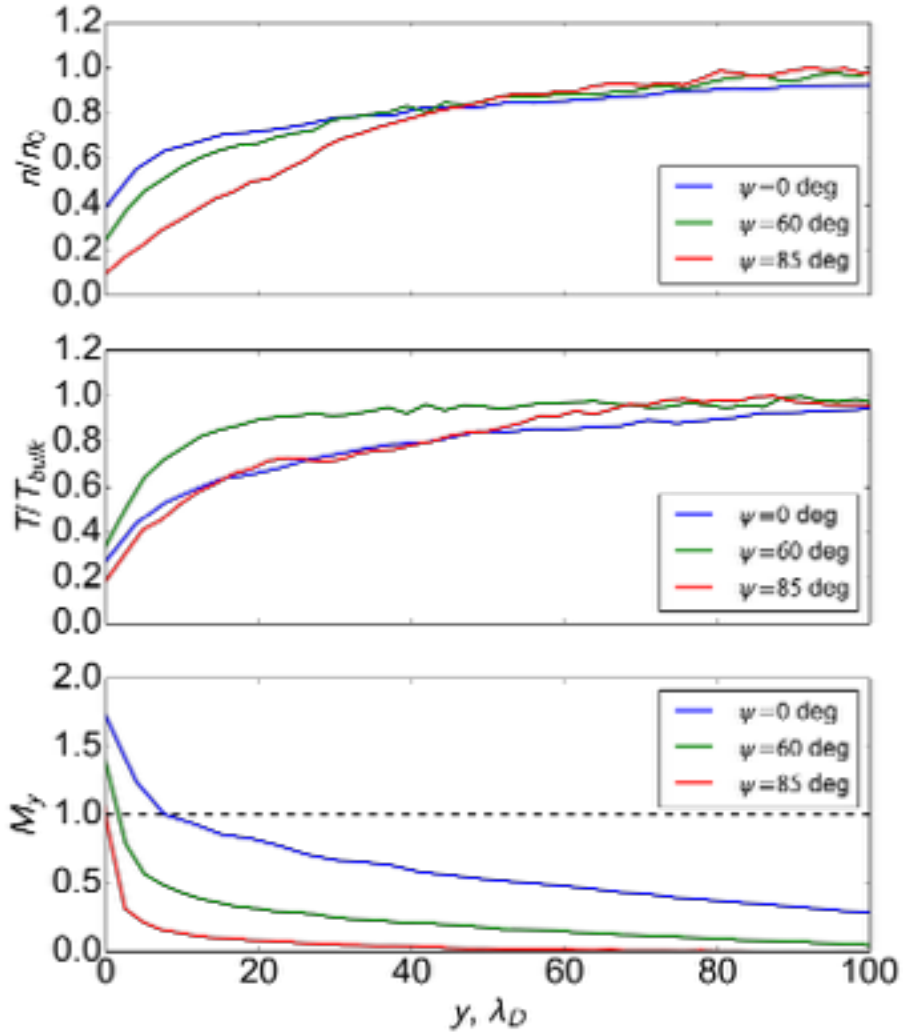

Ion Energy-Angle Distributions @ Wall

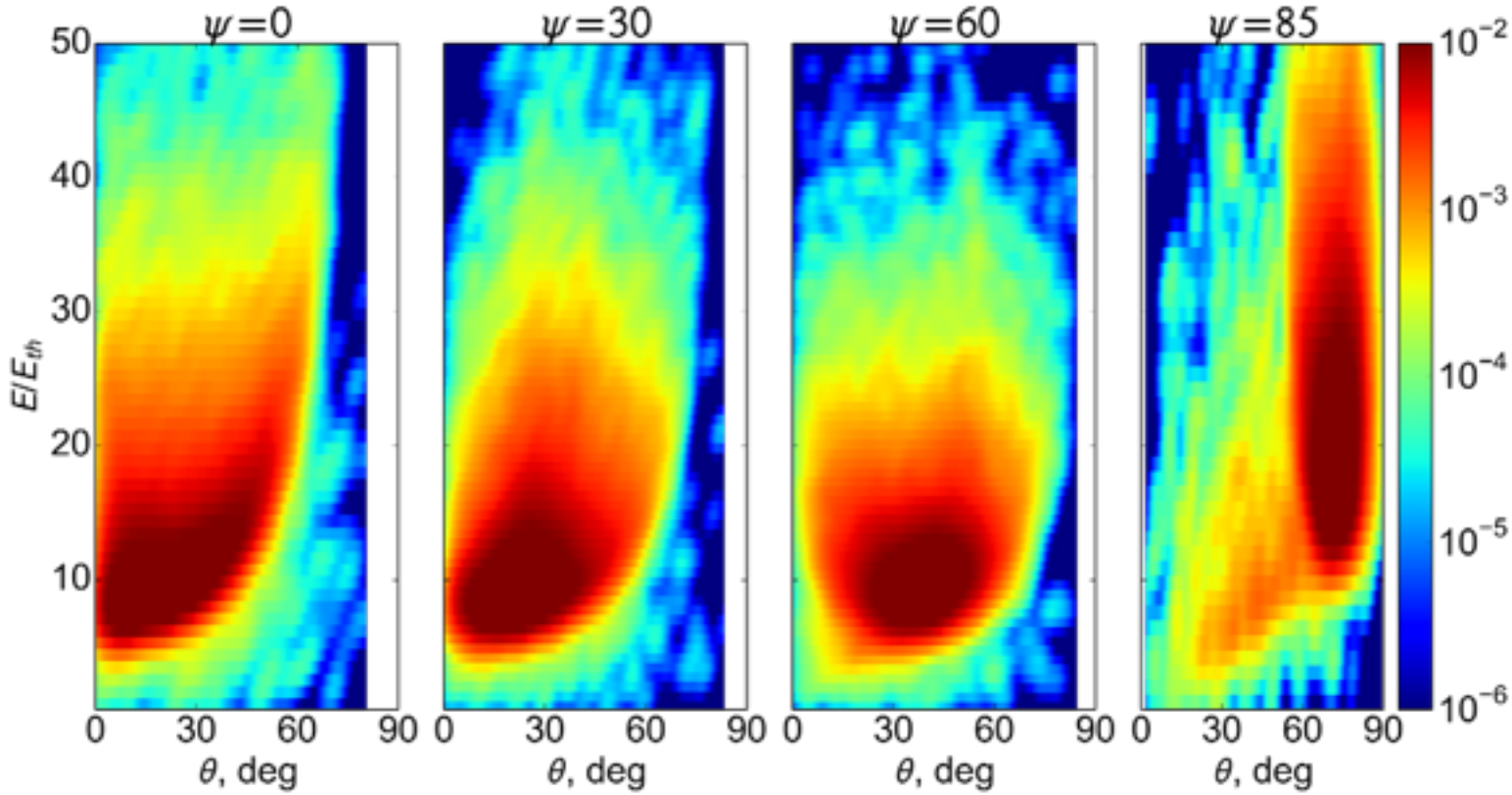

At θ_0=0 deg (normal incidence), the energy-angle peak occurs at ~5E_{th} and ~15-18 degrees; surprisingly, most of the ions do not arrive at normal incidence! All the ion energy is contained within 45-50E_{th}, over three decades of amplitude of the distribution

Increasing the B-field inclination causes a shift in both energies *and* angles at the wall;
At grazing angles the angular distribution is narrower along the angular coordinate, but it becomes wider along the energy coordinate

Fluid vs. PIC - Comparison of Energy Peaks

Fluid Ion Kinetic Energy Ei at Sheath Entrance (SE)

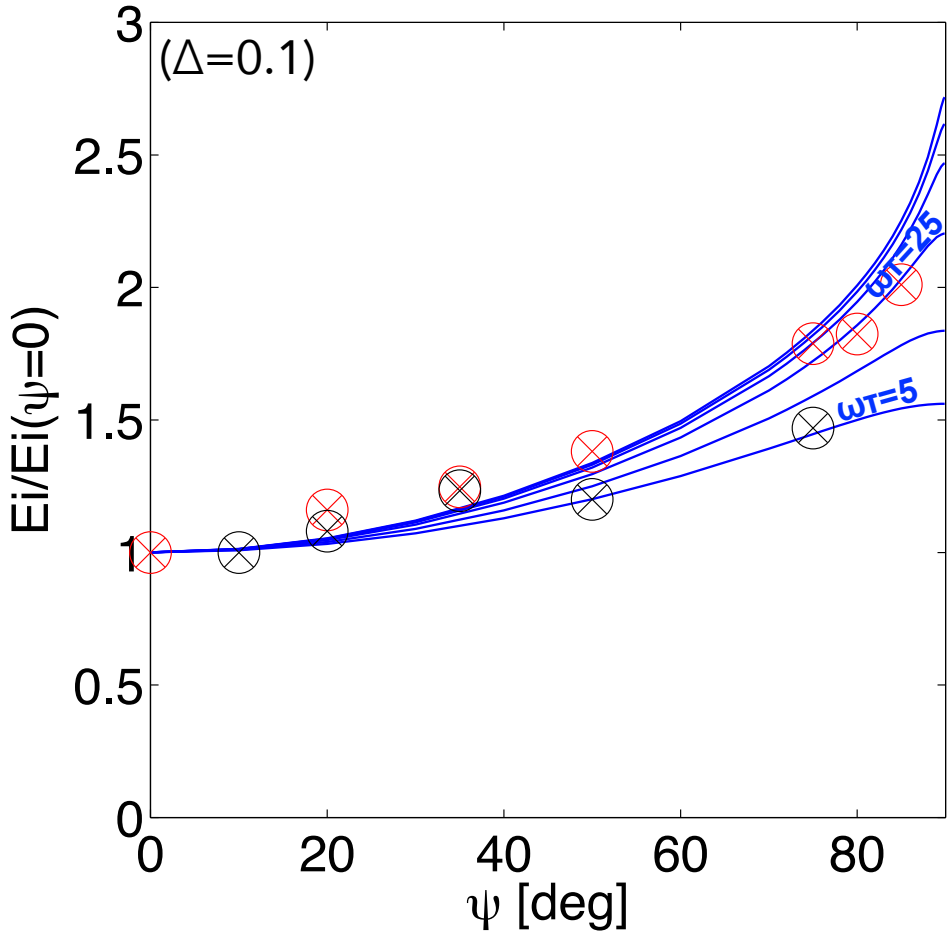

Ion Energy-Angle Distributions @ Wall

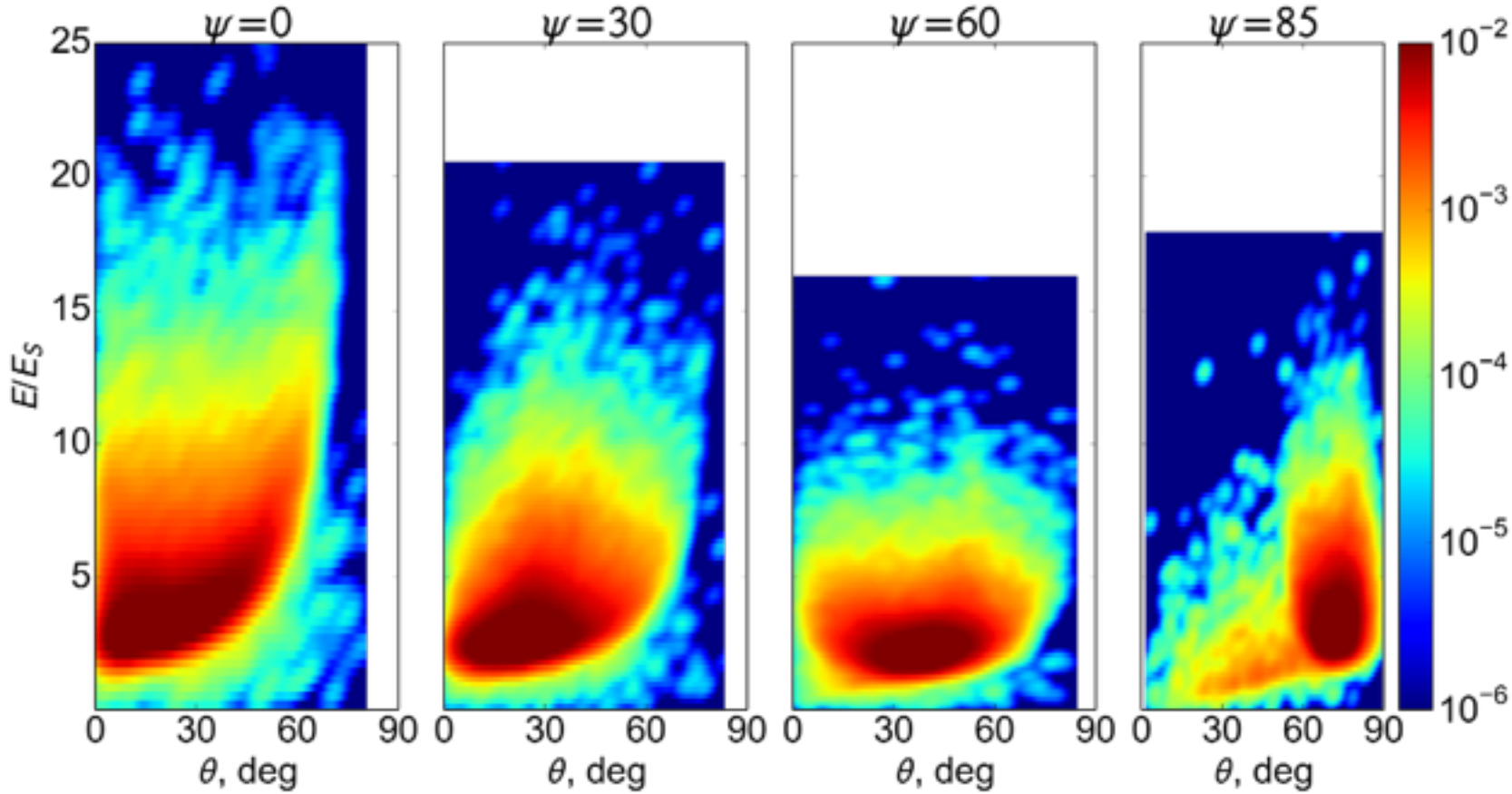

Scaling is now with respect to the total acoustic energy of the plasma

Ion Energy Distribution Functions @ Wall

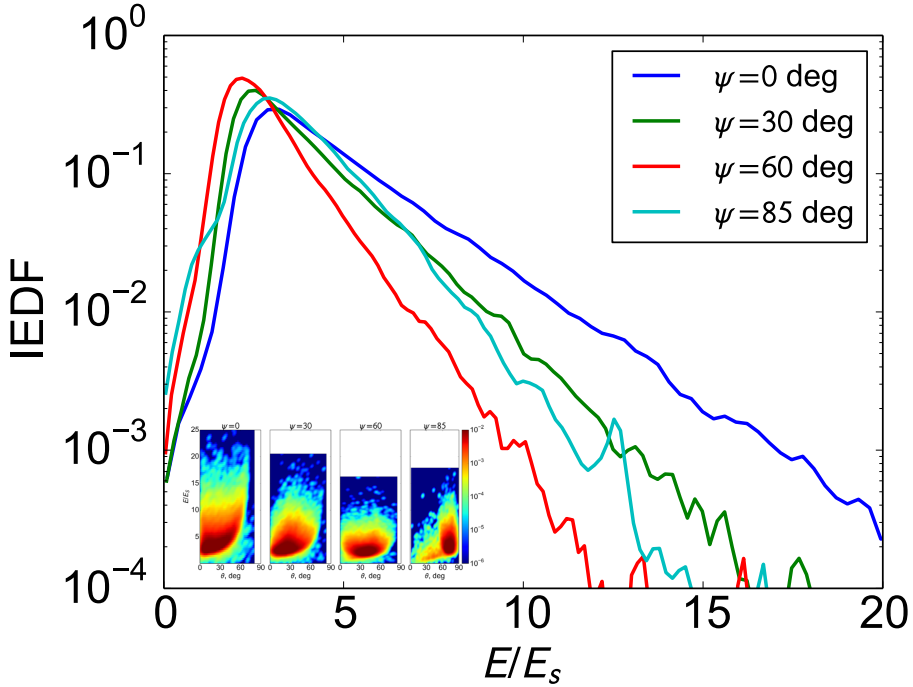

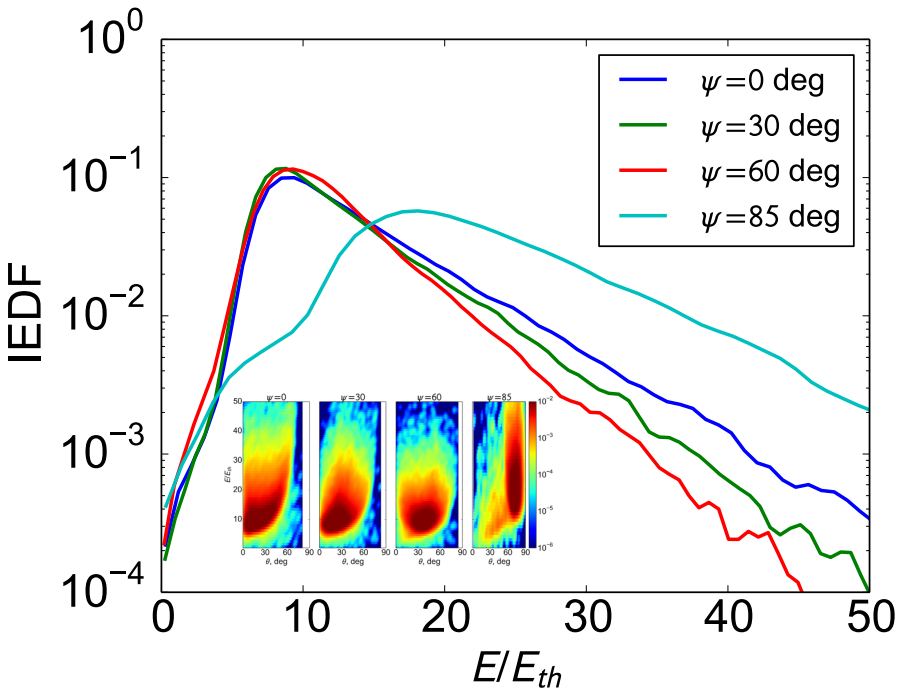

Influence of a Lorentz Scattering Operator

- The addition of a Lorentz scattering operator does not change the trends of the IEDF, as expected by diffusion on a sphere of v = constant
- Here "Intermediate collisions" and "High Collisions" are intended w.r.t the ion cyclotron and electron cyclotron frequencies

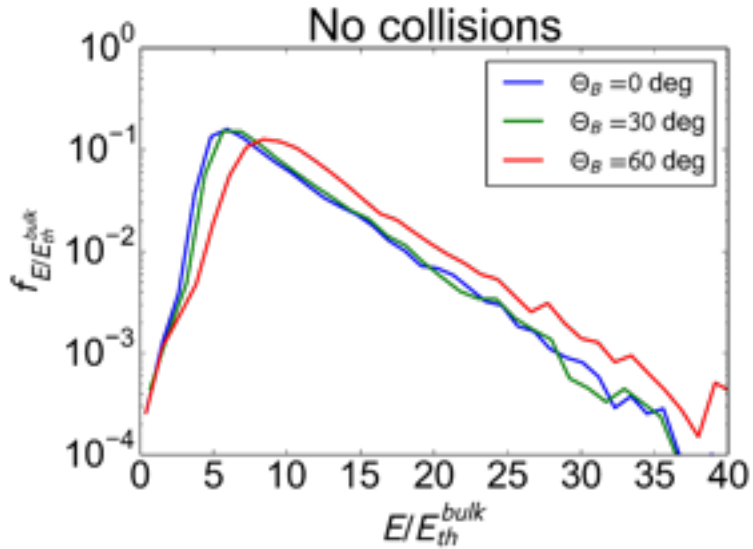

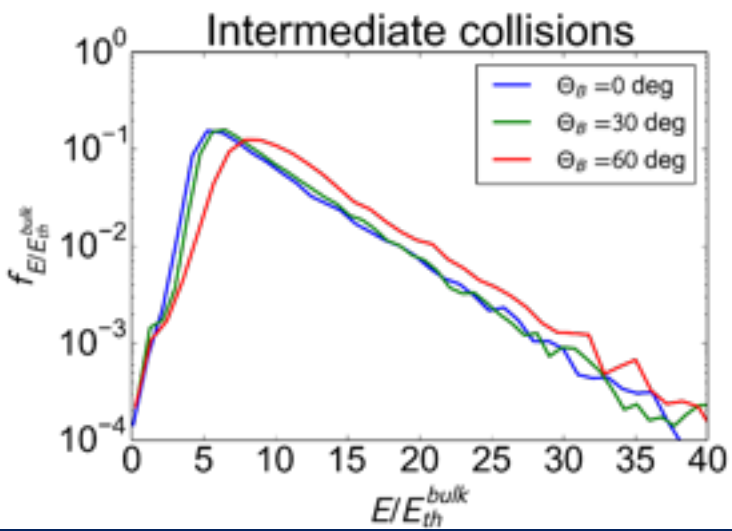

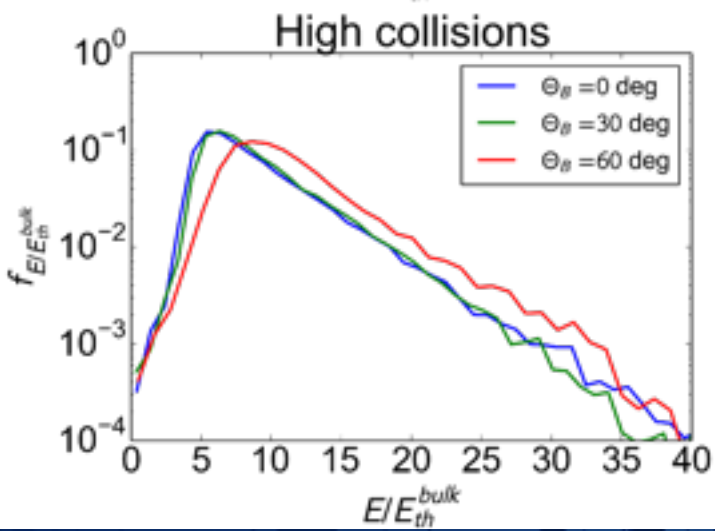

Ion Angular Distribution Functions at the Wall

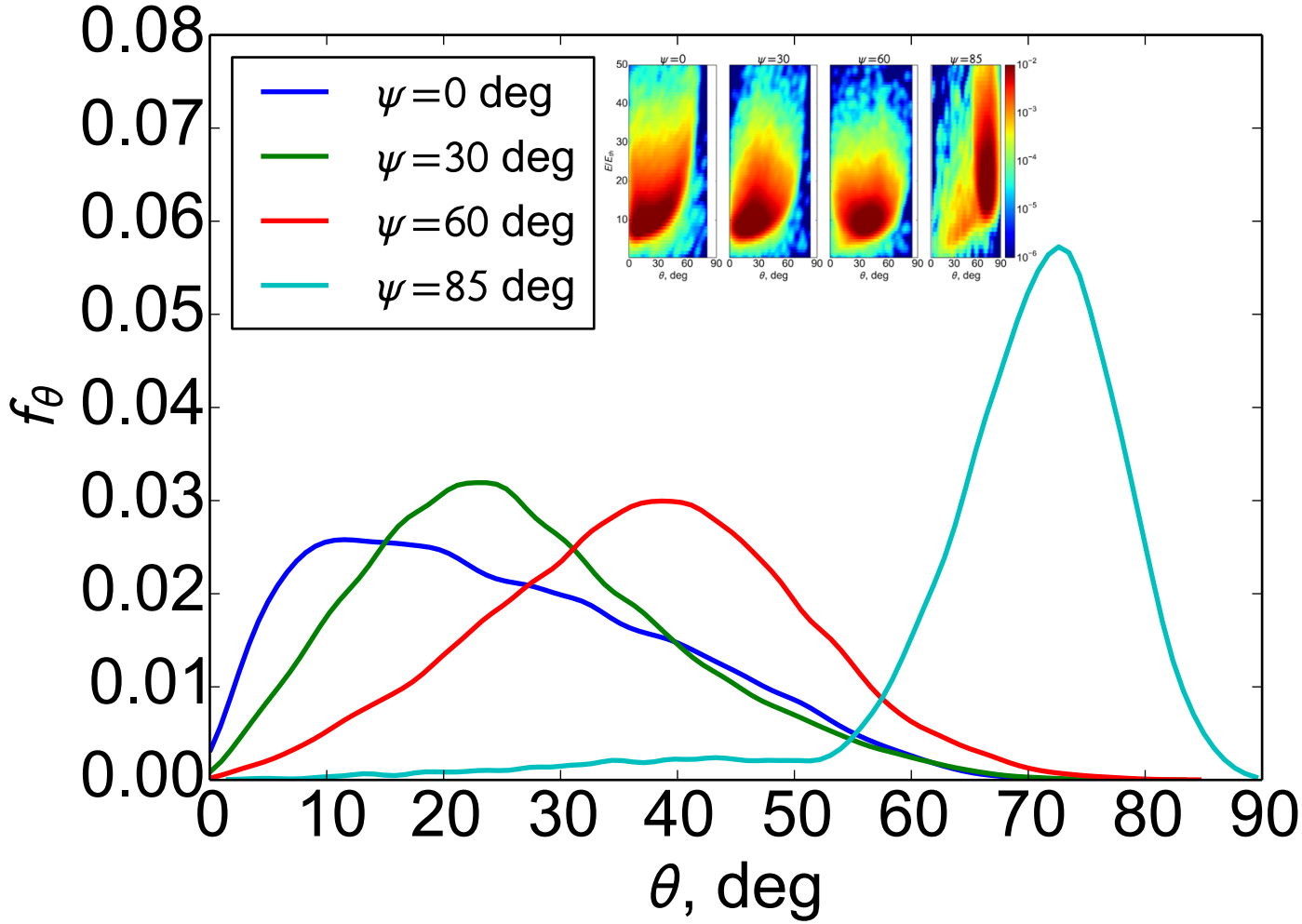

Influence of a Lorentz Scattering Operator

- The peak of $f(\theta_w)$ is independent than the collision rate of the Lorentz operator
- In order to quantify the peak trend, we have conducted a larger set of simulations at slightly-reduced resolution

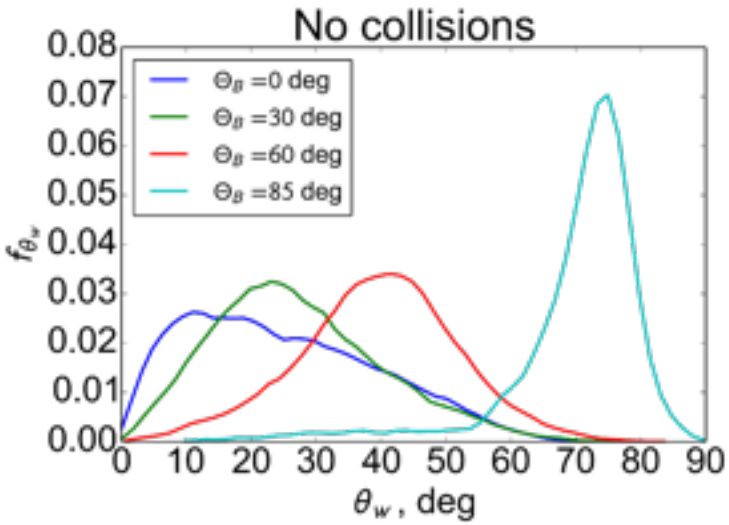

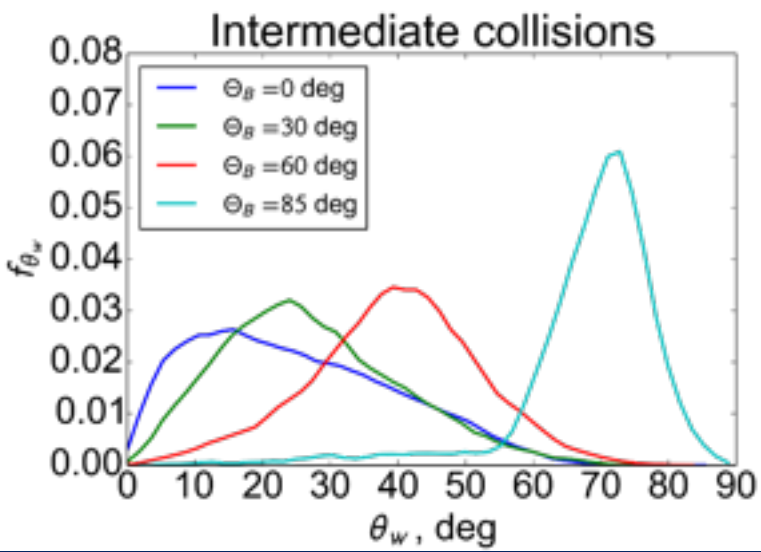

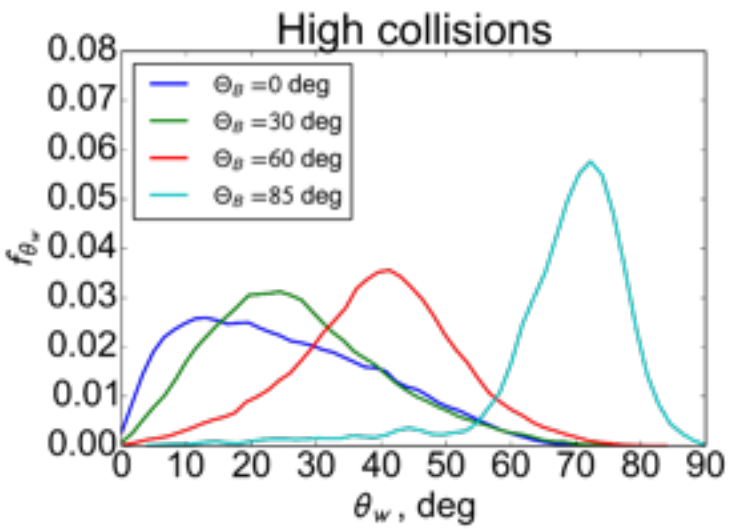

Peak angles of the IADF's vs. ψ

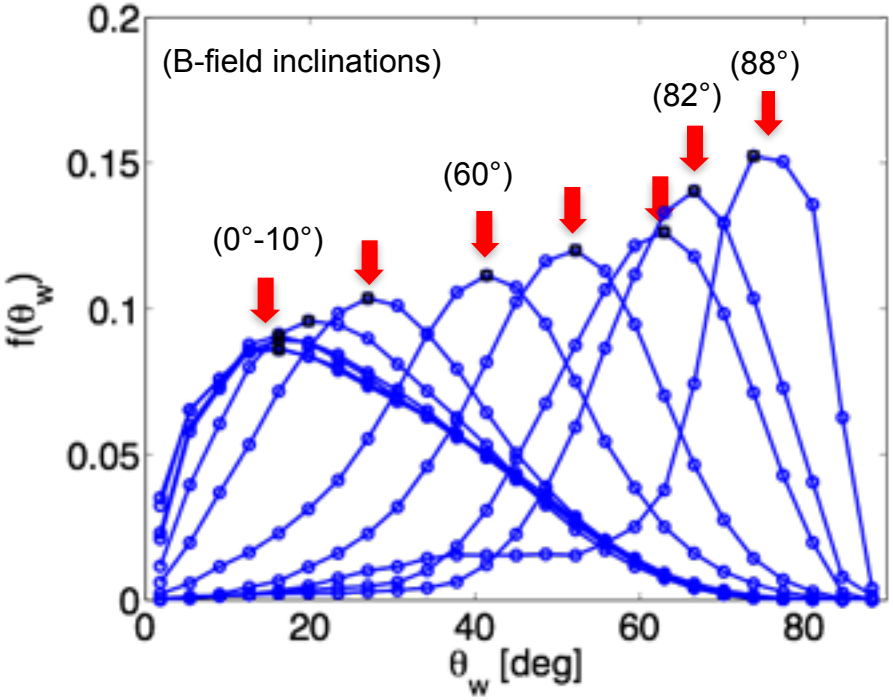

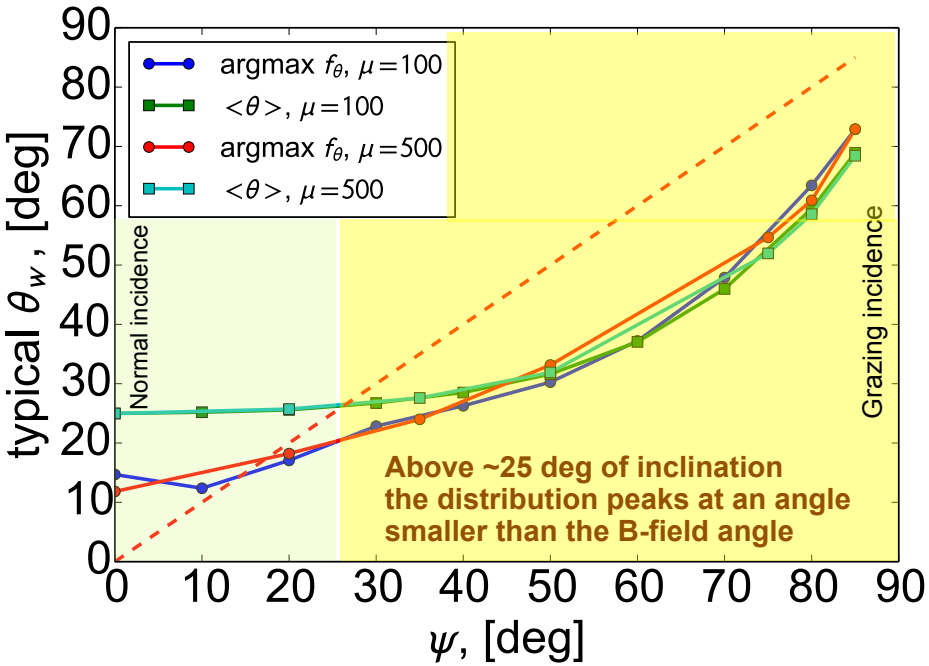

Ions 3D features at the time of impact

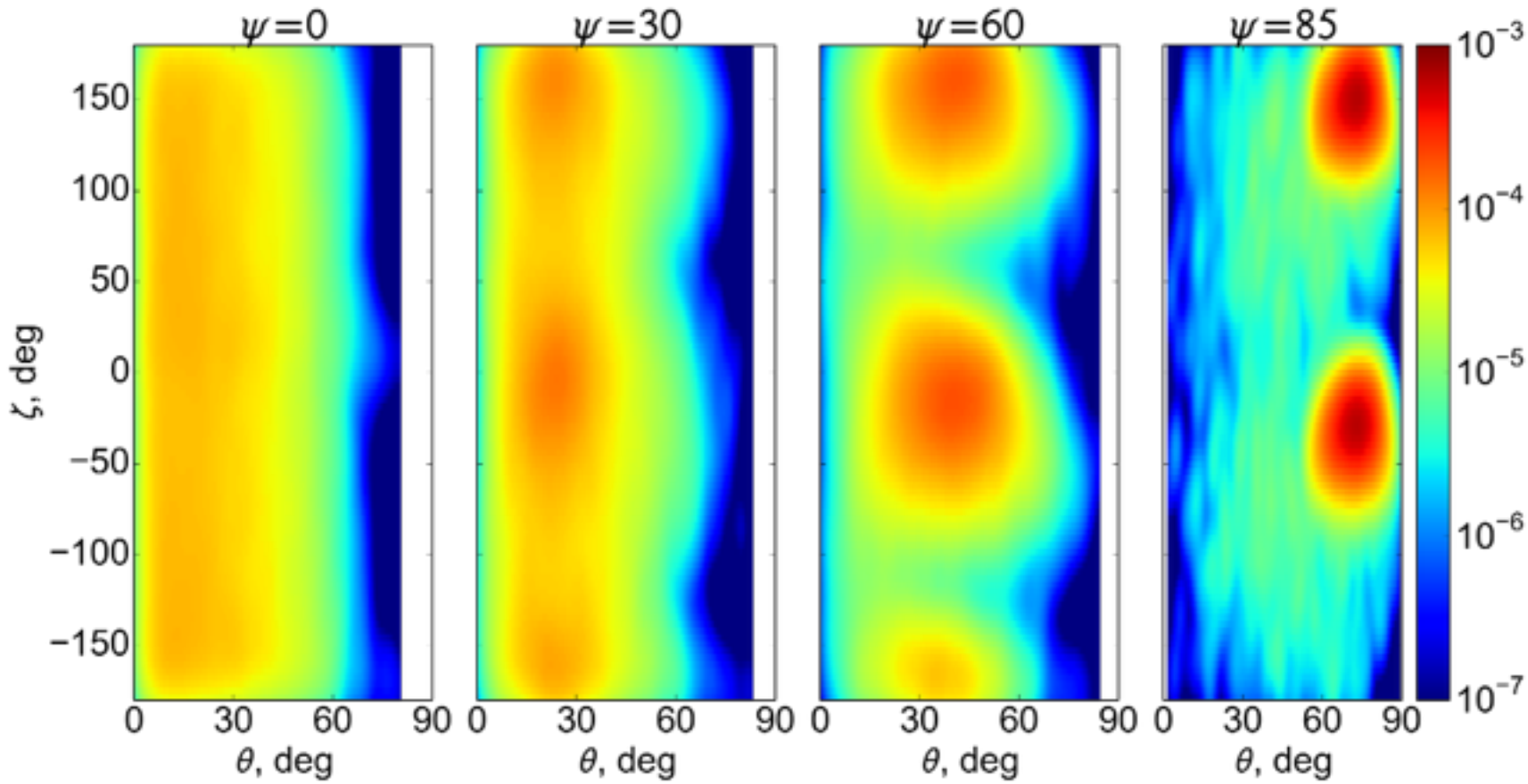

Kinetic IEADs affect how EIRENE evaluates the impurity release at the surface

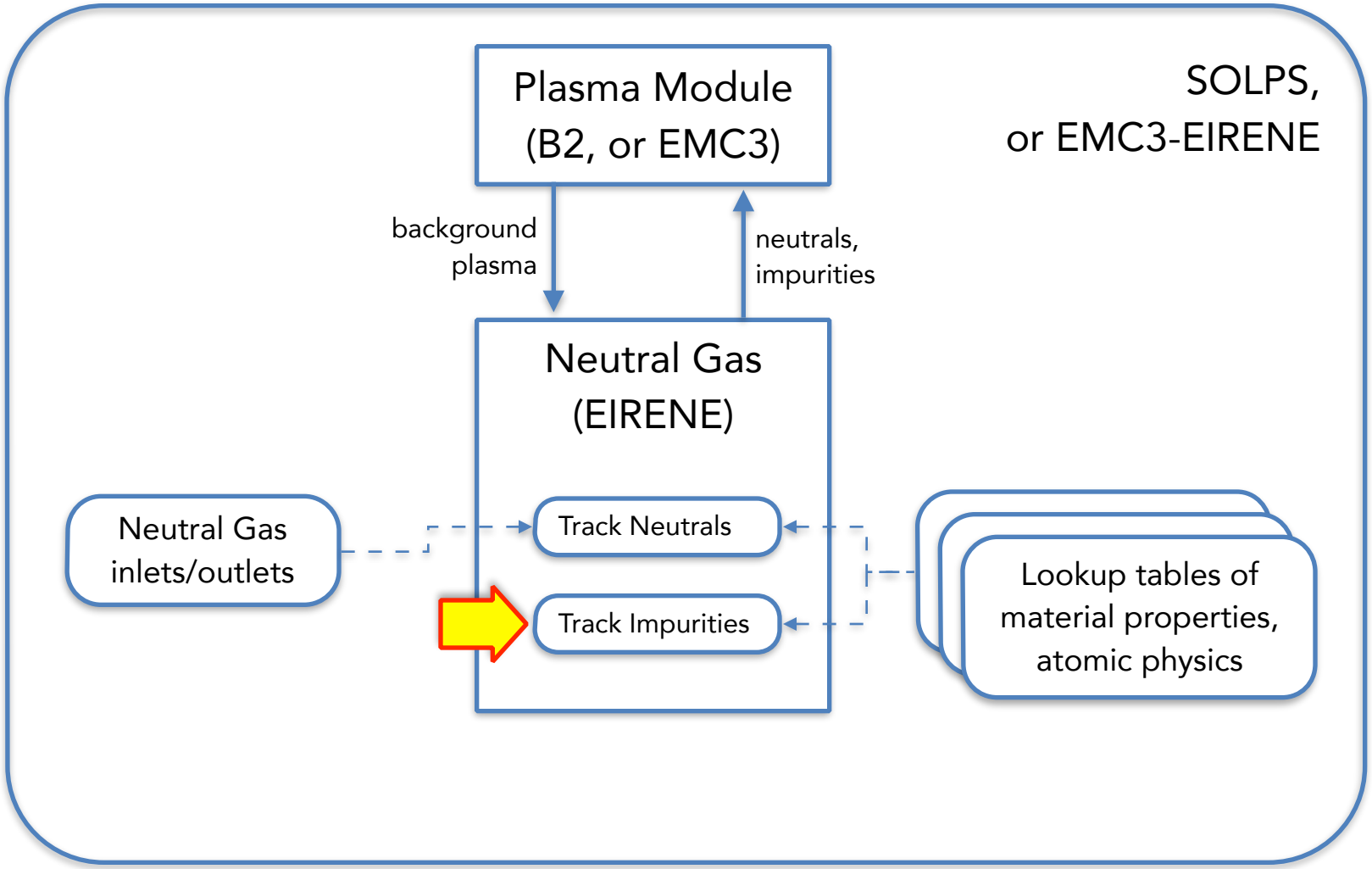

The wall properties are considerably affected not only by E, but also by θ! Examples for $Y(E,\theta)$

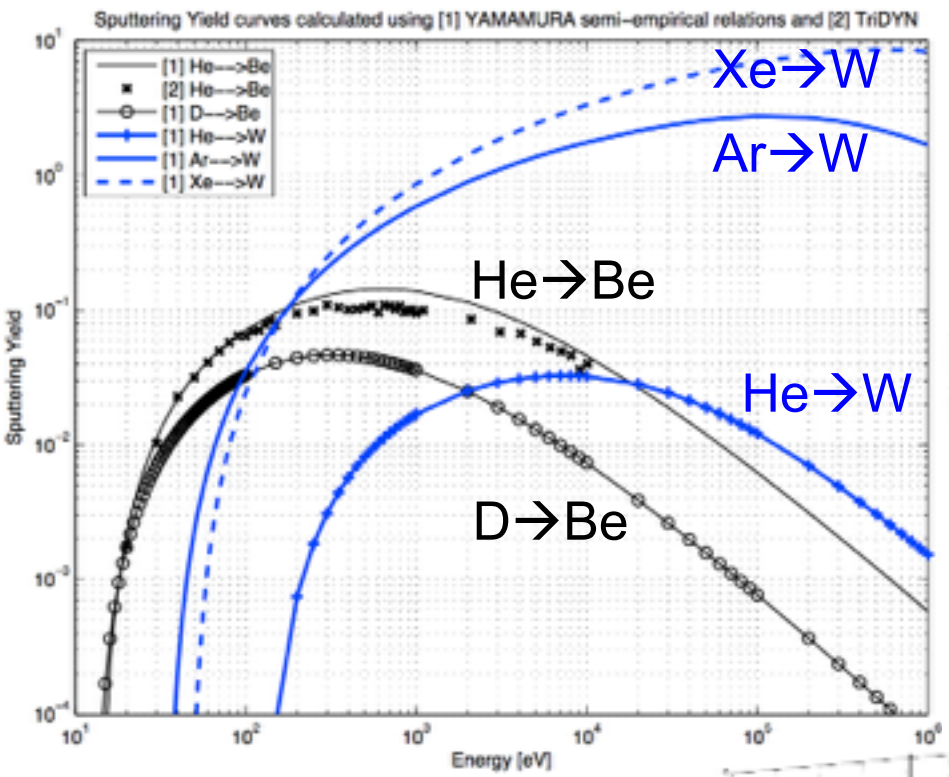

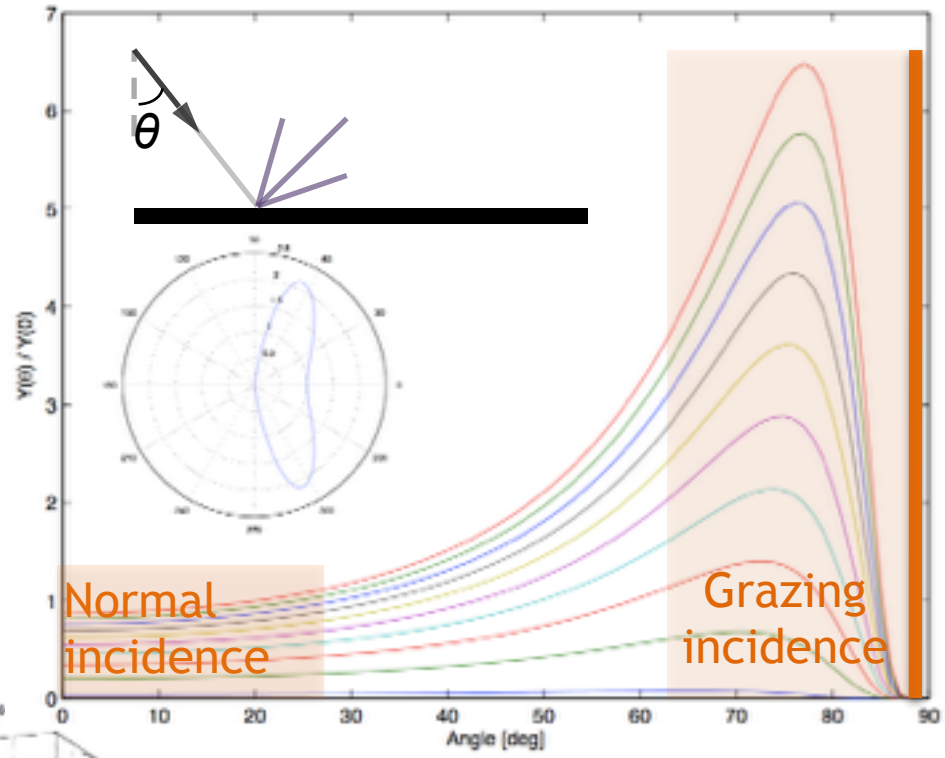

E

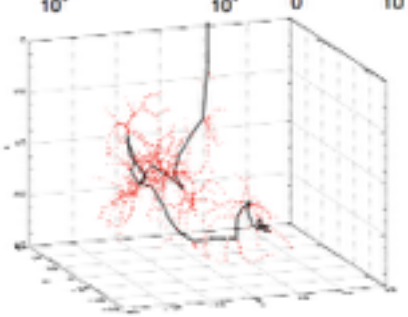

θ

Release of Material Particles (e.g. Y, δ_e) and wall reflection coefficients depend on $f(E_w)$ and $f(\theta_w)$ @ wall

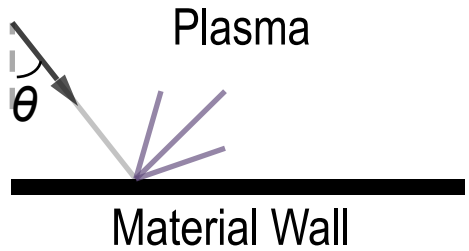

$$\boxed{Y = Y(E,\theta)}$$

Nuclear stopping cross-section

$$Y(E,0) = 0.042 \frac{Q(Z_2)\alpha^*(M_2/M_1)}{U_s} \frac{S_n(E)}{1+\Gamma k_e \epsilon^{0.3}} \left[1 - \sqrt{\frac{E_{th}}{E}}\right]^s$$

Surface binding energy

Reduced Energy

Lindhard electronic stopping coefficient

$$\frac{Y(E,\theta)}{Y(E,0)} = f\left(\theta, U_s, \frac{a_{screen}}{R_0}, \psi(E)\right)$$

Ratio of Lindhard screening length and average lattice constant

Release of Material Particles (e.g. Y, δ_e) and wall reflection coefficients depend on $f(E_w)$ and $f(\theta_w)$ @ wall

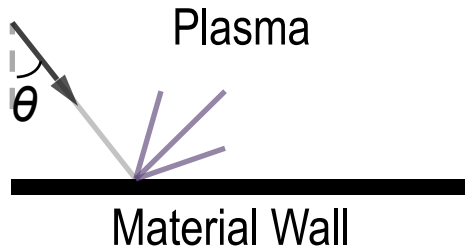

$$\boxed{Y = Y(E,\theta)}$$

Nuclear stopping cross-section

$$Y(E,0) = 0.042 \frac{Q(Z_2)\alpha^*(M_2/M_1)}{U_s} \frac{S_n(E)}{1+\Gamma k_e \epsilon^{0.3}} \left[1 - \sqrt{\frac{E_{th}}{E}}\right]^s$$

Surface binding energy

Reduced Energy

Lindhard electronic stopping coefficient

in SOLPS:

$$Y(E,0) = Q \cdot s(E) \cdot \left(1 - \left(\frac{E_{th}}{E}\right)^{2/3}\right) \cdot \left(1 - \frac{E_{th}}{E}\right)^2$$

$Y(E,0)$ of He->Be from BCA, low energy range

Sputtering of Be by normal incident He ions

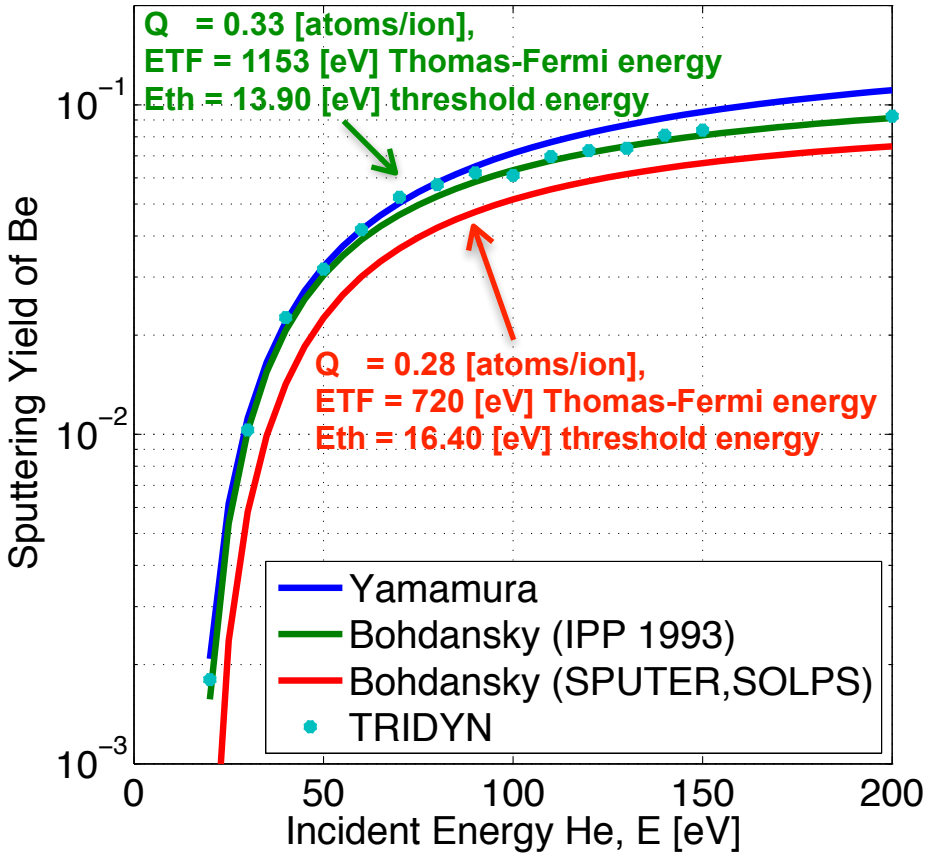

Experimental Data

Target	Projectile	Angle	Symbol	$E_{th}(eV)$	Q(atoms/ion)
Be/JET	He	0	△	13.9	0.707

Calculated Data

Target	Projectile	Angle	Symbol	$E_{th}(eV)$	Q(atoms/ion)
Be	He	0	▲	13.9	0.330
Be	Ne	0	■	40.2	1.90
Be	Ar	0	♦	48.1	2.96

ecktein_IPP_9_82

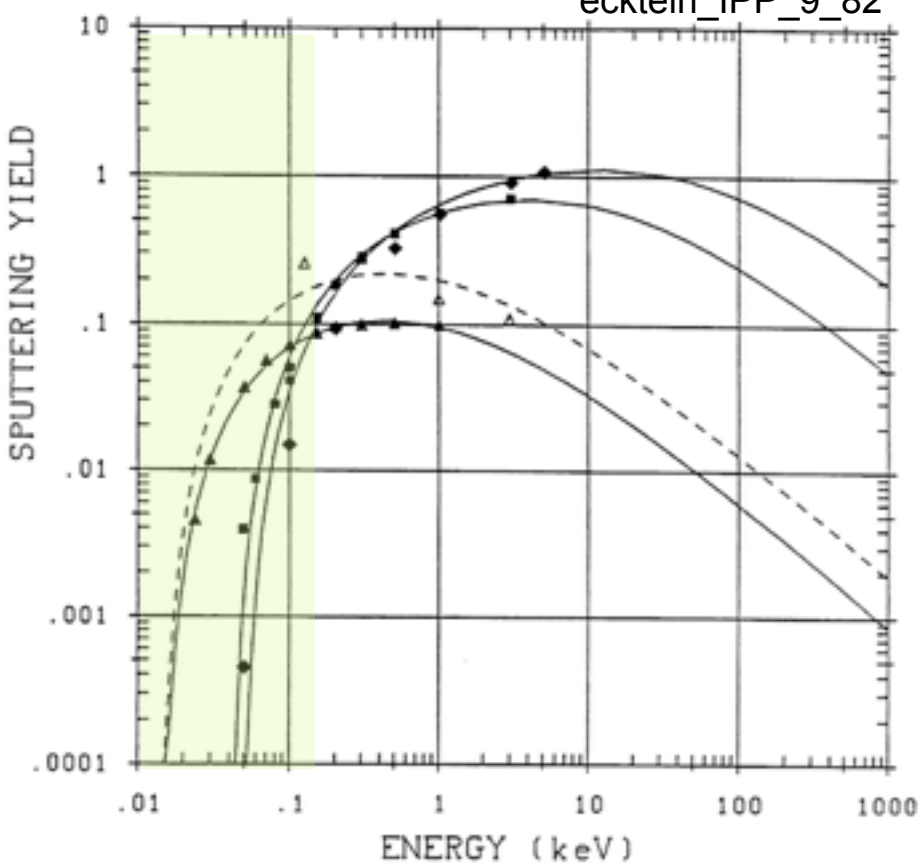

$Y(E,0)$ of He->Be from BCA, low energy comparison with PISCES-B data

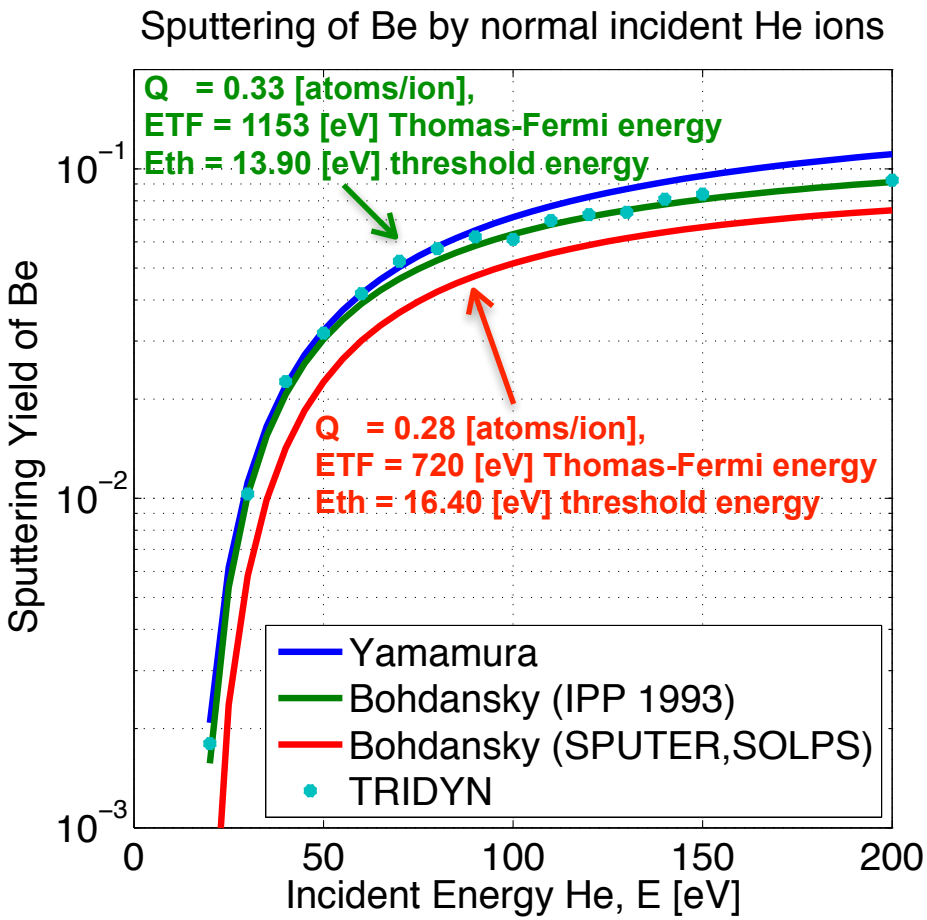

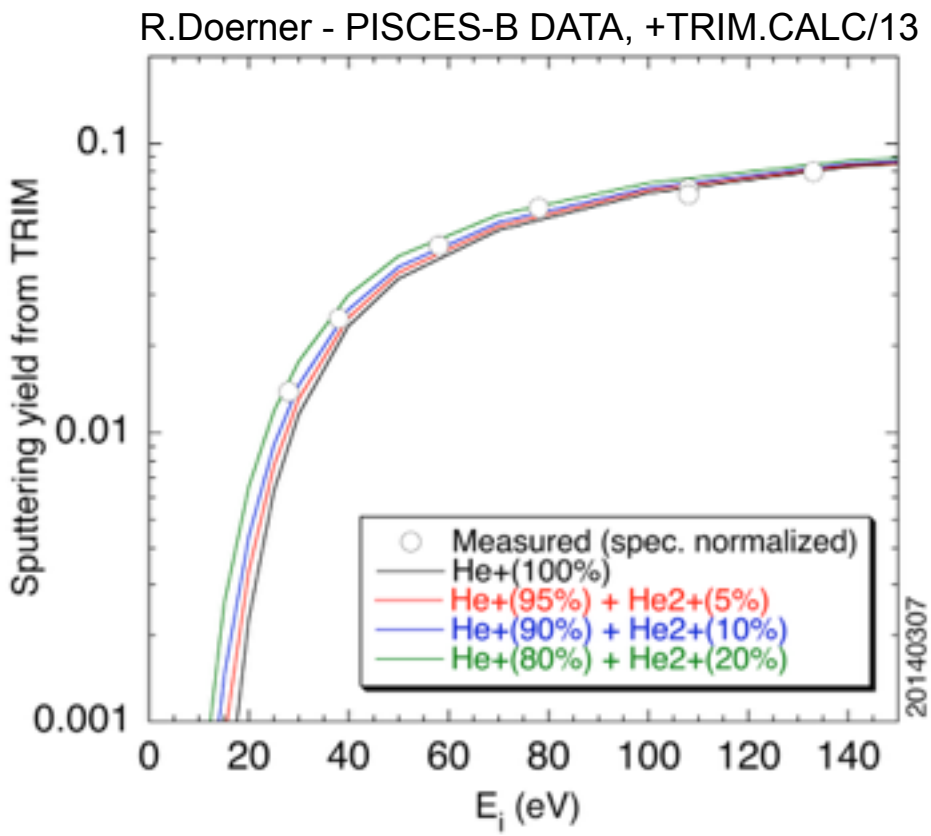

$Y(E,0)$ of He->Be, effect of surface roughness using fractal description of surface orientation

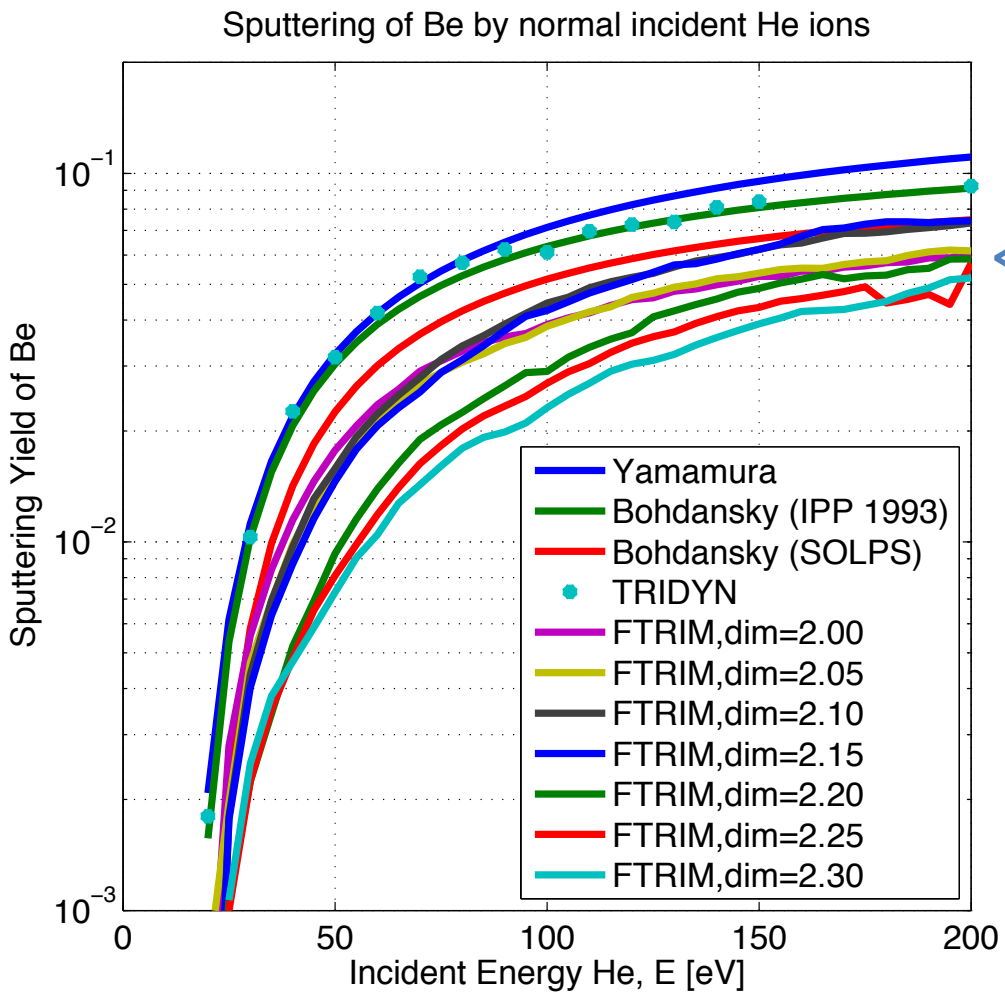

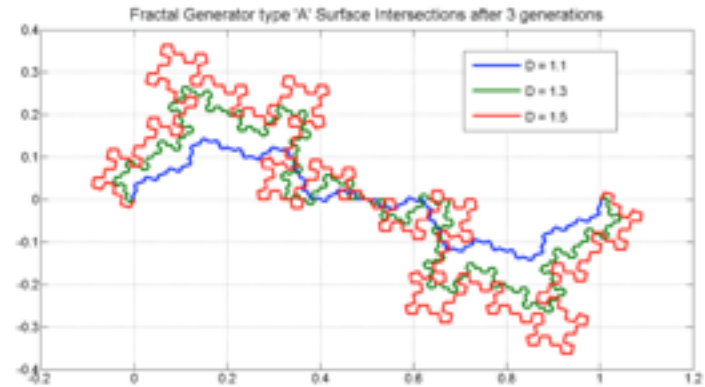

All the curves can be fitted using a "Bodhansky-like" formula with 2 free parameters *Q*, E_{th}:

$$Y(E,0) = Q \cdot s(E) \cdot \left(1 - \left(\frac{E_{th}}{E}\right)^{2/3}\right) \cdot \left(1 - \frac{E_{th}}{E}\right)^{2}$$

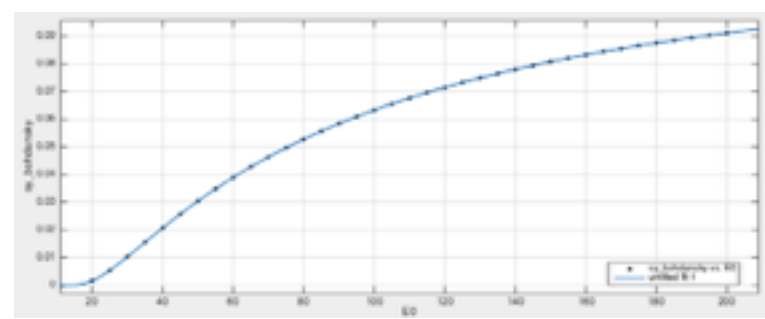

Y(*E*,0) of He->Be, effect of surface roughness using fractal description of surface orientation

Results from fitting using a Bodhansky-like formula; non-linear least-squares fitting trend of the 2 free parameters *Q* [atoms/ions], E_{th} [eV] vs. Fractal dimension

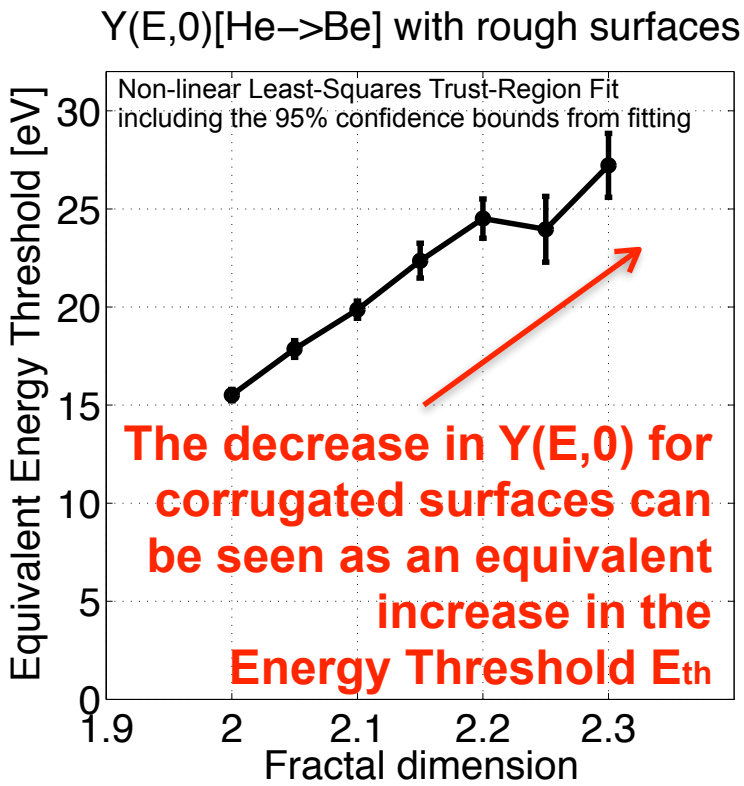

The decrease in Y(E,0) for corrugated surfaces can be seen as an equivalent increase in the Energy Threshold E_{th}

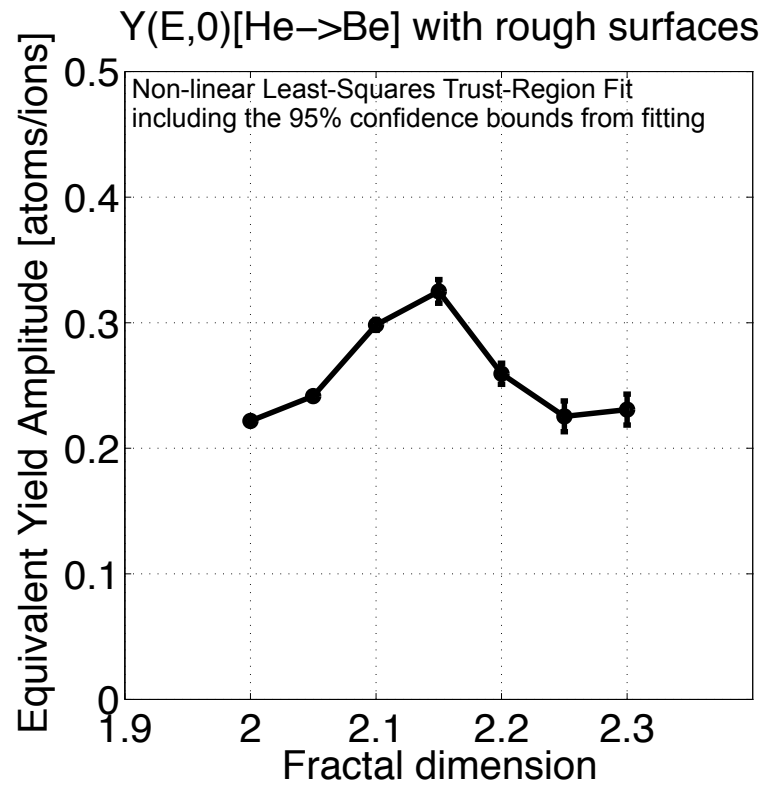

Increasing Surf.Roughness

The fractal description of the surface roughness can be included in plasma edge codes

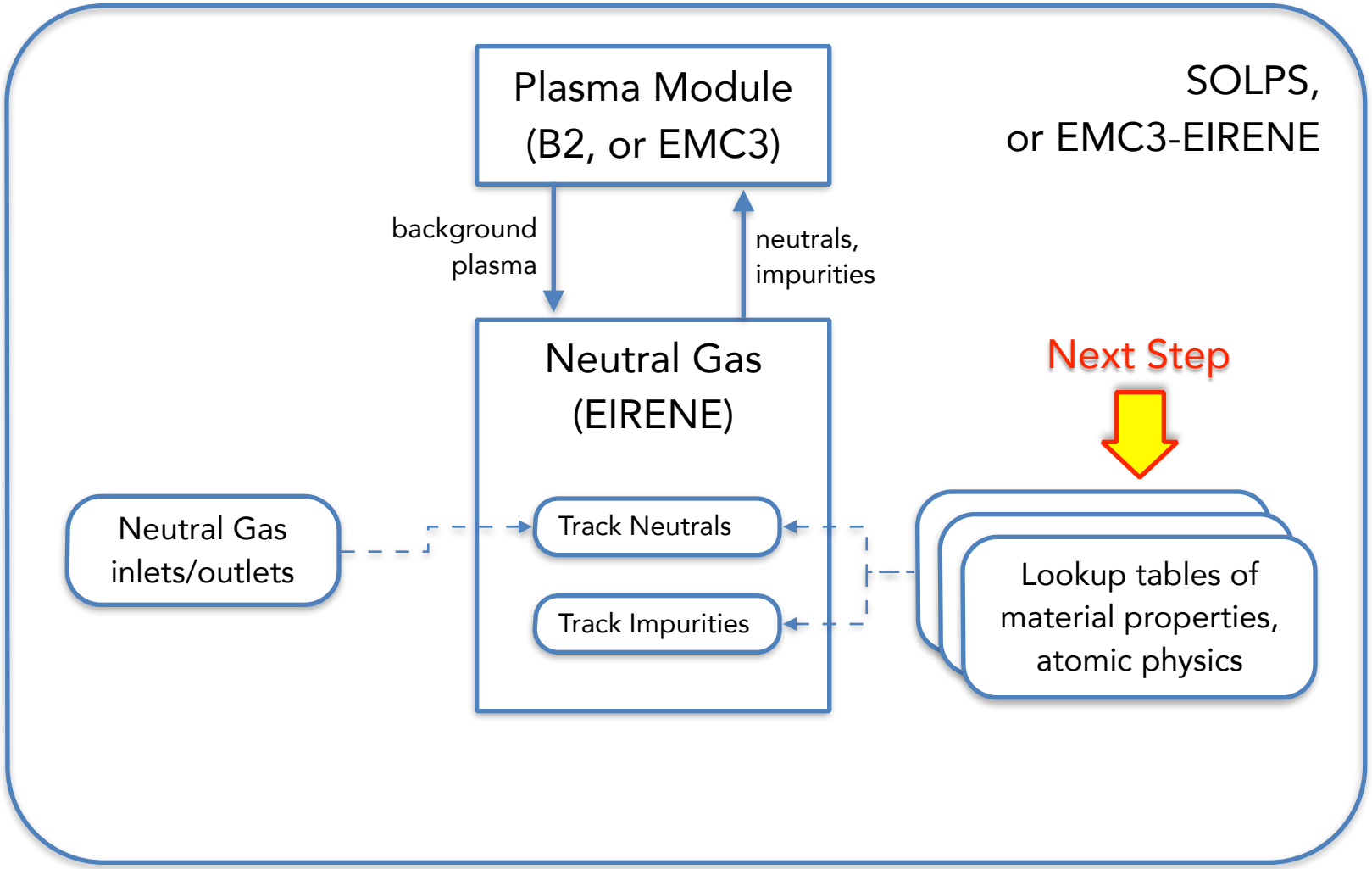

Conclusions

- Ion Energy-Angle Distribution Function at the boundary of a magnetized plasma is strongly dependent on both the magnitude and inclination of the magnetic field
- The peak angle of the ions at wall is always different than the B-field angle
- Proper treatment of the wall response requires the IEADF for the calculation of the material properties
- Progress on BCA codes done with the development of fractal-TRIDYN and

Thanks!